Partial decay widths and form factor implementation for the simulation of the Λ_c^+ decays in SHERPA

Sven Schiffner
geboren am 28.10.1994 in Sebnitz

Institut für Kern- und Teilchendphysik
Fachrichtung Physik
Fakultät Mathematik und Naturwissenschaften
Technische Universität Dresden
2017

Eingereicht am 24. Mai 2017

1. Gutachter: Dr. Frank Siegert
2. Gutachter: Prof. Dr. Michael Kobel

Summary

Abstract
English:

Abstract
Deutsch

Contents

1 Introduction

One of the big questions of mankind is, why are we here. And the correspondending question is in physics is, why exists more matter than anti-matter in the universe. This thesis can't clear the question but it can be a part of the big picture.

The `LHC` (Large Hadron Collider) is one of the biggest experiments of humanity. This accelerator collides proton with protons, lead nuclei with protons or lead nuclei with lead nuclei. One detector of this big apparatus is the `LHCb`. The `LHCb` is a try to find the answer of the above question. It examines assymetries in the decay of matter and anti-matter mainly for lead-lead-collissions. And so deviations from the Standard Model. The Standard Model is a theory that describes the fundamental interactions between and the elementary particles itself very well. These deviations can result in additions to the Standard Model to consider a asymmetry between matter and anti-matter. And so lead to an answer for the matter surplus. For this the results from the experiment has to be compared to the theoratical results. But simulations are needed for the theoratical results. This comes from the different interactions that happens through a particle collision. A lot of particles are created and decay. On of the simulation tools is `Sherpa`. This program use Monte-Carlo techniques to obtain results.

One possible baryon that can be created is the Λ_c^+. It is the lightest baryon that contains a charm quark. The charm quark is like the up quark that builds together with the down quark neutrons and protons but heavier.

For a good comparison between the experimental results and the theoratical simulations is it important to implement as much particles in the simulation as possible. This leads in a better description of the reaction and so in better theoretical results.

This thesis has the goal to improve the simulation through a better implementation of the Λ_c^+ decays.

2 Basic Physical Principles

2.1 Baryons

A Baryon is a subatomic particle. It is composite and contains three quarks. The Baryons form together with the mesons the class of the hadrons. Mesons are composed of two quarks, one quark and one antiquark.

Protons and neutrons which are the components of our normal matter are baryons. These are the lightest baryons. The proton is made of two up quark and one down quark. The neutron contains two down quark and one up quark.

All observed events so far feature that the number of baryons in a reaction is observed. To use this in calculations every quark get the baryon number $B = 1/3$ and every anti-quark $B = -1/3$. In a decay from a baryon ($\sum B = 1$) the final products has to be a baryon ($\sum B = 1$) or two baryons ($\sum B = 2$) and an anti-baryon ($\sum B = -1$) and so on.

2.1.1 Λ_c^+ Baryon

The Λ_c^+ has a mass of $2286.46 \pm 0.14\text{MeV}$[3] and a mean life time of $(2.00 \pm 0.06) \cdot 10^{-13}\text{s}$[3]. It is one of the lightest charmed baryons and is made of one up, down and charm quark. His charge is $+1$ of the electron charge[3].

2.2 Decays

Decays are processes with one particale in the initial state and n particles in the final state for n= 2,3,.... The decayed particle mustn't be in the final state. This makes the difference to rediation processes. The decay process can always be transformed in the rest mass frame of the Decayer and so the summation over the energy of all particles in the final state has to be the rest energy of the decaying particle.

A decay process or more general a transision process is characterized through Fermi's golden rule(2.1).

$$\Gamma_{fi} = 2\pi |T_{fi}|^2 \rho(E_i) \qquad (2.1)$$

In equation(2.1) T_{fi} is the transition matrix element and $\rho\left(E_i\right)$ is the density of states. The result is the transition rate Γ_{fi}.In natural units the unit of the transition rate is GeV^{-1}.

For decay process the only one intial is possible, the decayer and f is often labeled as i in literature. And so Fermi's golden rule becomes to equation (**??**).

$$\Gamma_i = 2\pi|T_i|^2\rho\left(E\right) \tag{2.2}$$

The Γ_i is called partial decay width. And is characteristic value for a decay process. The sum over all partial decay widths is called total decay width(2.3).

$$\Gamma = \sum_i \Gamma_i \tag{2.3}$$

The total width(2.3) is an criterion for the lifetime of the decaying particle. The lifetime(**??**) of the particle in natural units is the inverse of Γ.

$$\tau = \frac{1}{\Gamma} \tag{2.4}$$

The branching ratio(2.5) is the probability to decay in a specific final state. It can be calculated with the partial and total decay width.

$$BR(i \to f) = \frac{\Gamma_f}{\Gamma} \tag{2.5}$$

The formula (2.5) use the same indices like equation(2.1).

2.3 Weak Decay

A weak decay is the transition of a particle through the weak interaction. An elementary particle that is possibly part of an composite can in this way decay to a $W^\pm$-Boson and an correspondending part. But the W-Boson only couple to lef-handed fundamental partciles and right-handed fundamental anti-particles. The spinor for the weak interaction than looks like (2.6). There the upper have isospin -1/2 and the lower isospin +1/2.

$$\begin{pmatrix} \nu_e \\ e \end{pmatrix}_L, \begin{pmatrix} \nu_\mu \\ \mu \end{pmatrix}_L, \begin{pmatrix} d \\ u \end{pmatrix}_L, \begin{pmatrix} s \\ c \end{pmatrix}_L, \text{ etc.} \tag{2.6}$$

In (2.6) only the important particles are shown.

The value for a $W^\pm$ propagator is $\propto \frac{1}{q^2-m_W^2}$. But in most process the transfered momentum is much lower compared to the Mass of the $W^\pm$ boson because it is the mass difference of the initial particle and the final particle that are connected through the $W^\pm$ vertex. This leads to an estimation there the propagator becomes to $\propto \frac{1}{m_W^2} \propto G_F$. G_F is the Fermi constant for

the weak interaction and the process looks like a one to three vertex because $W^\pm$ boson is not stable and decays in other particles.

The measurement of leptons are mostly very accurate in a detector and the calculation of the transisition matrix element becomes easier for leptonic decays only this decays are considered. For the Λ_c^+ exists the following Feynman diagram(2.1). The Λ_c^+ can decay in a neutron or a Lambda as baryon and a positron or anit-muon as lepton plus the correspondending neutrino to observe the lepton number.
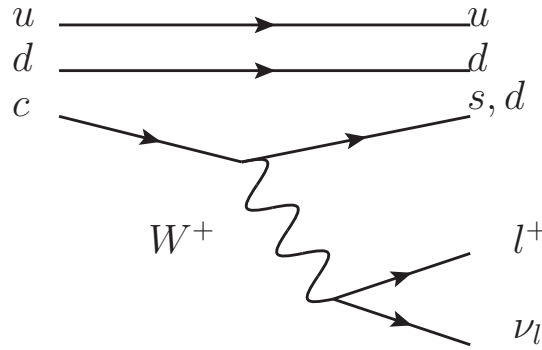

Figure 2.1: Semileptonic decay modes of the Λ_c^+ into a neutron (udd) or a Λ (uds), an positron or an anti-muon and the correspondending neutrino (own graphic)

2.4 V-A current

The value of a Vertex where two pertinent leptons transforms into a $W^\pm$ boson is $-i\frac{g}{2\sqrt{2}}\gamma^\mu\left(1-\gamma^5\right)$. If the sum is splitted, the the term without γ^5 is called vector and the part with the γ^5 axial-vector through the geometrical effect of the γ-matrix. The transition from quarks needs an additional factor V_{if}. i is the quark and in the initial state and f the quark in the final state. The factor comes from the CKM-matrix[2]. The matrix from [2] is shown in (2.7).

$$V_{CKM} = \begin{bmatrix} 0.97434^{+0.00011}_{-0.00012} & 0.22506 \pm 0.00050 & 0.00357 \pm 0.00015 \\ 0.22492 \pm 0.00050 & 0.97351 \pm 0.00013 & 0.0411 \pm 0.0013 \\ 0.00875^{+0.00032}_{-0.00033} & 0.0403 \pm 0.0013 & 0.99915 \pm 0.00005 \end{bmatrix} \tag{2.7}$$

With the general Feynman rules for vertices and propagators the transition matrix element becomes to (2.8) like in [11, Eq. 1].

$$T = \frac{G_F}{\sqrt{2}}V_{Qq}\bar{u}_l\gamma^\mu\left(1-\gamma^5\right)u_{\nu_l}\langle B(p',s')|J_\mu|\Lambda_c(p,s)\rangle \tag{2.8}$$

The B in (2.8) stands for the neutron or Λ. The current J_μ can be splitted in a vector-axial and an axial part $J_\mu = V_\mu - A_\mu$ like in (2.9).

$$\langle B(p', s')|V_\mu|\Lambda_c(p, s)\rangle = \bar{u}(p', s') \left(F_1(q^2)\gamma_\mu + F_2(q^2)\frac{p_\mu}{m_{\Lambda_c}} + F_3(q^2)\frac{p'_\mu}{m_B} \right) u(p, s)$$

$$\langle B(p', s')|A_\mu|\Lambda_c(p, s)\rangle = \bar{u}(p', s') \left(G_1(q^2)\gamma_\mu + G_2(q^2)\frac{p_\mu}{m_{\Lambda_c}} + G_3(q^2)\frac{p'_\mu}{m_B} \right) \gamma^5 u(p, s) \quad (2.9)$$

The F_i and G_i are form factors for the transition. They are specific for the initial and final baryons and describe the different behavior of the quarks in a bound state in contrast to the free decay. The functional behavior of these form factors is related to $q^2 = (p - p')^2$.

2.5 Monte-Carlo basics

The `Sherpa` software use Monte-Carlo methods to calcullate the dynamics of the process for the phase space integration of the partial width. To understand this method Fermi's golden rule(2.1) has to be written as an integral. This integral can be ontained from the density of states. A formula like [12, Eq. 2.38] is the result of this equation. The differential dacay rate is an important part because with Monte-Carlo the integral can be performed. For this a point in the phase space is diced. The differential decay rate $d\Gamma$ is calculated. If the Ratio between the differential decay rate and the maximum decay rate is bigger as a random number between zero and one the event is accepted. This points will be collected and form the integral and so the decay rate at the end.

3 Methods and Implementation

3.1 Decays Data

`Sherpa` use for the decays from all kinds of particles the decay channels and branching ratios from the `Decaysdata.db`. This database has to be updated manually with data from the Particle Data Group (PDG) because there exists no automation for this work. Also data from other sources are included, e.g. EvtGen.

Good results need actual data. The first part is to update the branching ratios and deyays. For the $\Xi(1690)$ was an implementation not possible because there exists to few events about futher decays. The conclusion of different events needs a lot of attention. For some events like $\Lambda_c^+ \to \Sigma(1385)^- + \pi^+ + \pi+$ only the channel $\Sigma(1385) \to \Lambda + \pi$ was recognized. So a division with the BR($\Sigma(1385) \to \Lambda + \pi$) was needed because `Sherpa` handle further decays and consider all different decays of the $\Sigma(1385)^-$. Table (A.1) was revealed with this knowledge. An abstract is visible in (3.1).

Table 3.1: Extract of the changes in the Decays.dat from the Λ_c^+

Status	Outgoing Part.	BR(Delta BR)[Origin]	Decay
Modes with nucleons/Deltas			
old	2212,-311	0.023(0.006)[PDG]	$\Lambda_c^+ \to P^+ + K_b$
new	2212,310	0.0158(0.0008)[PDG]	$\Lambda_c^+ \to P^+ + K_s$
old	2212,-321,211	0.028(0.008)[PDG]	$\Lambda_c^+ \to P^+ + K^- + \pi^+$
new	2212,-321,211	0.035(0.004)[PDG]	
old	2212,-311,111	0.033(0.010)[PDG]	$\Lambda_c^+ \to P^+ + K_b + \pi$
new	2212,310,111	0.0199(0.0013)[PDG]	
old	2212,-311,221	0.012(0.004)[PDG]	$\Lambda_c^+ \to P^+ K_b + \eta$
old	2212,211,211,-211,-211	0.018(0.012)[PDG]	$\Lambda_c^+ \to P^+ + \pi^+ + \pi^+ + \pi^- + \pi^-$
new	2212,211,211,-211,-211	0.0023(0.0015)[PDG]	
S = 0			
old	2212,9010221	0.0028(0.0019)[PDG]	$\Lambda_c^+ \to P^+ + f(0980)$
new	2212,9010221	0.0035(0.0023)[PDG]	
S = 0			
deleted	2212,211,-211	0.0007(0.0007)[PDG]	$\Lambda_c^+ \to P^+ + \pi^+ + \pi^-$

S = 0			
old	2224,-321	0.0086(0.003[PDG]	$\Lambda_c^+ \rightarrow \Delta(1232)^{++} + K^-$
new	2224,-321	0.0109(0.0025)[PDG]	
Modes with hyperons			
old	3122,211	0.0107(0.0028)[PDG]	$\Lambda_c^+ \rightarrow \Lambda + \pi^+$
new	3122,211	0.0130(0.0007)[PDG]	
created	3122,211,111	0.071(0.0004)[PDG]	$\Lambda_c^+ \rightarrow \Lambda + \pi^+ + \pi$
created	3122,213	0.036(0.013)[PDG]	$\Lambda_c^+ \rightarrow \Lambda + \rho(770)^+$
S = 0			
old	3122,321	0.0005(0.00016)[PDG]	$\Lambda_c^+ \rightarrow \Lambda + K^+$
new	3122,321	0.00061(0.00012)[PDG]	
created	3112,211,211	0.021(0.004)[PDG]	$\Lambda_c^+ \rightarrow \Sigma^- + \pi^+ + \pi^+$
semileptonic modes			
old	3122,12,-11	0.021(0.006)[PDG]	$\Lambda_c^+ \rightarrow \Lambda + \nu_e + e^+$
new	3122,12,-11	0.036(0.004)[PDG]	
old	3122,14,-13	0.020(0.007)[PDG]	$\Lambda_c^+ \rightarrow \Lambda + \nu_\mu + \mu^+$
new	3122,14,-13	0.036(0.004)[PDG]	

In the case of $\Lambda_c^+ \rightarrow P^+\pi^+ + \pi^-$ was the decay already included in $\Lambda_c^+ \rightarrow P^+ + f(0980)$. K_b was removed from the PDG and only K_s exists. For $\Lambda_c^+ \rightarrow \Lambda + \eta + \pi^+$ give the difference between $\Lambda + \pi^- + \pi + \pi^+ + \pi^+$ and $\Sigma(1385)^+ + \eta$ the right value because an η decays in $\pi^+ + \pi^-$ and a $\Sigma(1385)$ to $\Lambda + \pi$. But the decay of the $\Sigma(1385)$ is a separate channel.

These decays are selected because the full list would be too long and so it is visible that some channel becomes likelier. But as an compensation other process has to become less probable. These process are in most cases very similiar and redistribution rests upon a better identification of the final decay states and a better particle reconstruction. One of the important changes is the increase of the branching ratios from the semileptonic decays by nearly 1%. Other important process that didn't changed are shown in table(3.2)

Table 3.2: Decays in a neutron in the Decays.dat from the Λ_c^+

Status	Outgoing Part.	BR(Delta BR)[Origin]	Decay
semileptonic modes			
old	2112,12,-11	0.003[EvtGen]	$\Lambda_c^+ \rightarrow n + \nu_e + e^+$
old	2112,14,-13	0.003[EvtGen]	$\Lambda_c^+ \rightarrow n + \nu_\mu + \mu^+$

The branching for these semileptonic decays only simulated. The reason is that most of the modern detectors can't detect neutrons very well. This comes from the neutral electric charge

and the long lifetime of the neutron. An improved measurement would be recommended because this processes are important for the form factor calculation. The neutron is often considered as the final decay state oif the Λ_c^+.

All these changes leads to a sum of all branching ratios from $87,98\%$. This is a pretty good value and very close to 100%. This means that the decay is very good abstracted.

3.2 Form Factor conversion

The two formulas in (2.9) show one popular parametrization for the V-A-Current another possible and popular writing is given in (3.1).

$$\langle B(p',s')|V_\mu|\Lambda_c(p,s)\rangle = \bar{u}(p',s')\left(f_1^V(q^2)\gamma_\mu + f_2^V(q^2)i\sigma_{\mu\nu}\frac{q^\nu}{m_{\Lambda_c}} + f_3^V(q^2)\frac{q_\mu}{m_{\Lambda_c}}\right)u(p,s)$$

$$\langle B(p',s')|A_\mu|\Lambda_c(p,s)\rangle = \bar{u}(p',s')\left(f_1^A(q^2)\gamma_\mu + f_2^A(q^2)\text{ß}\sigma_{\mu\nu}fracq^\nu m_{\Lambda_c} + f_3^A(q^2)\frac{q_\mu}{m_{\Lambda_c}}\right)\gamma^5 u(p,s)$$

$$(3.1)$$

In this notation is $q = p - p'$. A convsersion formula is now needed for the different parametrization of the current. The equations in [4, Eq. 15] give one direction for transformation. But most of the following form factors are in the form with p and p' and not with q. So the inversion of the given transformation would be the easiest way to get a decent formula. Another fact is that the current for an baryon baryon transition in `Sherpa` is already in the form like (2.9). The use of this parametrization let the implementation become a lot easier. The first step is to create a transformation matrix like in (3.2)

$$\begin{pmatrix} f_1^V \\ f_2^V \\ f_3^V \\ f_1^A \\ f_2^A \\ f_3^A \end{pmatrix} = \begin{bmatrix} 1 & \frac{m_{\Lambda_c}+m_B}{2m_{\Lambda_c}} & \frac{m_{\Lambda_c}+m_B}{2m_B} & 0 & 0 & 0 \\ 0 & -\frac{1}{2} & -\frac{m_{\Lambda_c}}{2m_B} & 0 & 0 & 0 \\ 0 & \frac{1}{2} & -\frac{m_{\Lambda_c}}{2m_B} & 0 & 0 & 0 \\ 0 & 0 & 0 & 1 & -\frac{m_{\Lambda_c}-m_B}{2m_{\Lambda_c}} & -\frac{m_{\Lambda_c}-m_B}{2m_B} \\ 0 & 0 & 0 & 0 & -\frac{1}{2} & -\frac{m_{\Lambda_c}}{2m_B} \\ 0 & 0 & 0 & 0 & \frac{1}{2} & -\frac{m_{\Lambda_c}}{2m_B} \end{bmatrix} \cdot \begin{pmatrix} F_1 \\ F_2 \\ F_3 \\ G_1 \\ G_2 \\ G_3 \end{pmatrix} \quad (3.2)$$

The block structure of the matrix is a mathemtaical manifestation of the independence of the

vector and axial-vector part. This matrix can be splitted in two equations(3.3).

$$
\begin{pmatrix} f_1^V \\ f_2^V \\ f_3^V \end{pmatrix} = \begin{bmatrix} 1 & \frac{m_{\Lambda_c}+m_B}{2m_{\Lambda_c}} & \frac{m_{\Lambda_c}+m_B}{2m_B} \\ 0 & -\frac{1}{2} & -\frac{m_{\Lambda_c}}{2m_B} \\ 0 & \frac{1}{2} & -\frac{m_{\Lambda_c}}{2m_B} \end{bmatrix} \cdot \begin{pmatrix} F_1 \\ F_2 \\ F_3 \end{pmatrix}
$$

$$
\begin{pmatrix} f_1^A \\ f_2^A \\ f_3^A \end{pmatrix} = \begin{bmatrix} 1 & -\frac{m_{\Lambda_c}-m_B}{2m_{\Lambda_c}} & -\frac{m_{\Lambda_c}-m_B}{2m_B} \\ 0 & -\frac{1}{2} & -\frac{m_{\Lambda_c}}{2m_B} \\ 0 & \frac{1}{2} & -\frac{m_{\Lambda_c}}{2m_B} \end{bmatrix} \cdot \begin{pmatrix} G_1 \\ G_2 \\ G_3 \end{pmatrix}
\tag{3.3}
$$

The matrices can be inverted if the determinant is unequal to zero. The determinant of both matrices are the same(3.4). This comes from the block structure with the zeroes in the first column.

$$
det(\dots) = \frac{m_{\Lambda_c}}{2m_B}
\tag{3.4}
$$

If the mass of the Λ_c^+ is nonzero than the matrices are invertible. And obviously is this true. The matrix for G_i is really in the fashion of the one for F_i. So the inverting has only be done ones. The matrices in (3.5) are calculated.

$$
\begin{pmatrix} F_1 \\ F_2 \\ F_3 \end{pmatrix} = \begin{bmatrix} 1 & \frac{3m_{\Lambda_c}+m_B}{4m_{\Lambda_c}} & -\frac{m_{\Lambda_c}+m_B}{4m_B} \\ 0 & -1 & 1 \\ 0 & -\frac{m_B}{2m_{\Lambda_c}} & -\frac{m_B}{2m_{\Lambda_c}} \end{bmatrix} \cdot \begin{pmatrix} f_1^V \\ f_2^V \\ f_3^V \end{pmatrix}
$$

$$
\begin{pmatrix} G_1 \\ G_2 \\ G_3 \end{pmatrix} = \begin{bmatrix} 1 & -\frac{3m_{\Lambda_c}-m_B}{4m_{\Lambda_c}} & \frac{m_{\Lambda_c}+m_B}{4m_B} \\ 0 & -1 & 1 \\ 0 & -\frac{m_B}{2m_{\Lambda_c}} & -\frac{m_B}{2m_{\Lambda_c}} \end{bmatrix} \cdot \begin{pmatrix} f_1^A \\ f_2^A \\ f_3^A \end{pmatrix}
\tag{3.5}
$$

And finally for every form factor a transformation formula(3.6) can be obtained.

$$
F_1 = f_1^V + \frac{m_{\Lambda_c}+m_B}{4}\left(\frac{3f_2^V}{m_{\Lambda_c}} - \frac{f_3^V}{m_B}\right)
$$

$$
F_2 = -f_2^V + f_3^A
$$

$$
F_3 = -\frac{m_B}{2m_{\Lambda_c}}\left(f_2^V + f_3^V\right)
$$

$$
G_1 = f_1^A + \frac{m_{\Lambda_c}-m_B}{4}\left(-\frac{3f_2^V}{m_{\Lambda_c}} + \frac{f_3^V}{m_B}\right)
$$

$$
G_2 = -f_2^A + f_3^A
$$

$$
G_3 = -\frac{m_B}{2m_{\Lambda_c}}\left(f_2^A + f_3^V\right)
\tag{3.6}
$$

The basic class FormFactor_Base from VA_B_B_FFs in `HADRONS++/Current_Library/VA_B_B.H`

is now extend with additional inline functions for the transformation. To use every time the same parametrization and didn't mix them.

3.3 Prevoius Form Factor implementation

At first it is important to know wich current parametrization is already used by the `VA_B_B.C` in `Sherpa`. With this information the right form can be choosen. For a natural transition between two baryons the different coefficient (3.7) are computed. A natural transition means that the decayer and the daughter baryon have the same parity.

$$c_{R1} = V_1 - A_1$$
$$c_{L1} = -V_1 - A_1$$
$$c_{R2} = V_2 - A_2$$
$$c_{L2} = -V_2 - A_2$$
$$c_{R3} = V_3 - A_3$$
$$c_{L3} = -V_3 - A_3 \tag{3.7}$$

V_i and A_i comes from the choosen from factor model. The following current(3.8) is sumed ove all possible helicities from the decaying h_0 and the daughter baryon h_1.

$$V_\mu = L_\mu(1, h_1, 0, h_0, c_{R1}, c_{L1}) +$$
$$\frac{p_{0,\mu}}{m_0} \cdot Y(1, h_1, 0, h_0, c_{R2}, c_{L2}) +$$
$$\frac{p_{1,\mu}}{m_1} \cdot Y(1, h_1, 0, h_0, c_{R3}, c_{L3}) \tag{3.8}$$

The definition of L_μ is given in [12, Eq. A.96] and the Y in [12, Eq. A.94]. They are visible again in (3.9).

$$L_\mu(1, h_1, 0, h_0, c_{R1}, c_{L1}) = \bar{u}(p_1, h_1)\gamma_\mu (c_{R1}P_R + c_{L1}P_L) u(p_0, h_0)$$
$$Y(1, h_1, 0, h_0, c_{R2}, c_{L2}) = \bar{u}(p_1, h_1) (c_{R2}P_R + c_{L2}P_L) u(p_0, h_0)$$
$$Y(1, h_1, 0, h_0, c_{R3}, c_{L3}) = \bar{u}(p_1, h_1) (c_{R3}P_R + c_{L3}P_L) u(p_0, h_0) \tag{3.9}$$

The projection operators that are used in (3.9) are defined in (3.10)

$$P_R = \frac{1}{2} (1 + \gamma_5)$$
$$P_L = \frac{1}{2} (1 - \gamma_5) \tag{3.10}$$

This all equations together form a current wich is similiar to {(2.9). This can also easily been seen through the signs of the γ_5 and the signs of the c_R and c_L. All other current parametrization have to be converted to observe the existing behavior.

3.4 Observables

Two observables are adapted from simulations of the BELLE experiment to compare the different form factors. The first is q^2 which is defined in (3.11).

$$q^2 = (p_{\Lambda_c} - p_B)^2 \tag{3.11}$$

And the second is the recoil of the W in (3.12)

$$w = \frac{p_{\Lambda_c}^2 + p_B^2 - (p_{\Lambda_c} - p_B)^2}{2 \cdot \sqrt{p_{\Lambda_c}^2} \cdot \sqrt{p_B^2}} \tag{3.12}$$

3.5 Form Factor Models

3.5.1 Covariant Confined Quark Model (CCQM)

The idea behind the covariant confined quark model is to use two loops Feynman diagrams with free quark propagators. The high energy behavior of the loop integrations is soften. This model was developed for mesons but is extended to baryons. It is also possible to successfully calculate tetraquark states with this theory.

For the transition to $\Lambda + l^+ + \nu_l$ the paper[7] was considered and for $n + l^+ + \nu_l$ the paper[6]. The parametrization of the form factor is given by (3.13)

$$f(q^2) = \frac{F(0)}{1 - as + bs^2} \text{ with } s = \frac{q^2}{m_{\Lambda_c}} \tag{3.13}$$

The parameters F(0), a and b are taken from the numerical results of [7].

3.5.2 Non relativistic Quark Model (NRQM)

Baryons with a heavy quark possesses a special symmetry. This symmetry is called heavy quark symmetry. This is based on works from Isgur and Wise. The name of the theory behind that is heavy quark effective theory (HQET). The main impact to the characteristics of the baryon results from the degrees of freedom of the light quarks and are independent from the degrees of freedom of the heavy quark.

This form factor can be used to calculate transitions to excited Λ baryons [9]. The parametriza-

tion of the form factors (3.14) a more complicated compared to the other ones.

$$F = \left(a_0 + a_2 q^2 + a_4 q_4\right) e^{-\frac{3 m_\sigma^2 p_\Lambda^2}{2 m_\Lambda^2 \alpha_{\lambda\lambda'}^2}}$$

$$p_\Lambda = \frac{1}{2 m_\Lambda} \lambda^{\frac{1}{2}}\left(m_{\Lambda_c}^2, m_\Lambda^2, q^2\right)$$

$$\lambda(x, y, z) = x^2 + y^2 + z^2 - 2xy - 2yz - 2zx \text{(triangle function)}$$

$$\alpha_{\lambda\lambda'} = \sqrt{\frac{\alpha_\lambda^2 + \alpha_{\lambda'}^2}{2}} \tag{3.14}$$

In equation(3.14) is m_σ the mass of the light quark obtained from [9, p. 13/I] and the α_λ are size parameters of the baryons from [9, p. 13/II].

3.5.3 Light-Cone Sume Rule (LCSR)

The light-cone sume rule is a vary famous technique in the class of QCD sum rules. The basic idea is that the vacuum condensates carry no momentum. The light-cone expansion is used with increasing twist. With this model was the transition into $\Lambda + l^+ + \nu_l$ in [8] computed. The parametrization(3.15) is through the same values for the first two axial-vector and vector form factors very simple

$$f_1^V = f_1^A$$

$$f_2^V = f_2^A$$

$$f_i(q^2) = \frac{f_i(0)}{a_2 s^2 + a_1 s + 1} \text{ with } s = \frac{q^2}{m_{\Lambda_c}} \tag{3.15}$$

$f_i(0)$, a_2 and a_1 are parameters of this parametrization. Only the first two factors are nonzero.

3.5.4 Relativistic Quark Model (RQM)

The relativistic quark model[5] is based on the diquark wave function and the baryon wave function of the bound quark-diquark state. The calculation were done with relativistic quasipotential equation of the Schrödinger type. All computation were relativistically done.
It can predict senmileptonic transitions into n as well as into Λ. The parametrization(3.16) was done until a very high order of the q^2.

$$F(q^2) = \frac{F(0)}{1 - \sigma_1 s + \sigma_2 s^2 + \sigma 31 s^3 + \sigma_4 s^4} \text{ with } s = \frac{q^2}{m_{\Lambda_c}} \tag{3.16}$$

3.5.5 QCD Sum Rule (QCDSR)

In the article [1] are nonperturbative aspects used. The approach of the QCD sum-rule is the expansion in local operators. Here is also the HQET usd to reduce the complexity. $\Lambda + l^+ + \nu_l$

is considered in the article.

In this Model two different parametrizations exists. The pole parametrization (3.17) is used like in the other models. But this pole parametrization is a lot simpler through relations between the form factors.

$$f_1^A = -f_1^V$$
$$f_2^A = f_2^V$$
$$f_i^V(q^2) = \frac{a_0}{a_1 - q^2} \tag{3.17}$$

The other form of the parametrization (3.18) is more complicated but through the exponential ansatz interesting.

$$f_1^A = -f_1^V$$
$$f_2^A = -f_2^V$$
$$f_1^V(q^2) = e^{\frac{q^2 - a_1}{a_0}}$$
$$f_2^V(q^2) = \frac{a_0}{a_1 - q^2} \tag{3.18}$$

The third form factor is in both cases zero.

4 Evaluation and Discussion

4.1 Decays data

With the old and the new decays data was made a simulation of the decay of the Λ_c^+. For a good statistic 100000000 events was used. This number is a good comparison between runtime and number of events per bin. In grpahics (4.1) and (4.2) you can see that the change of the
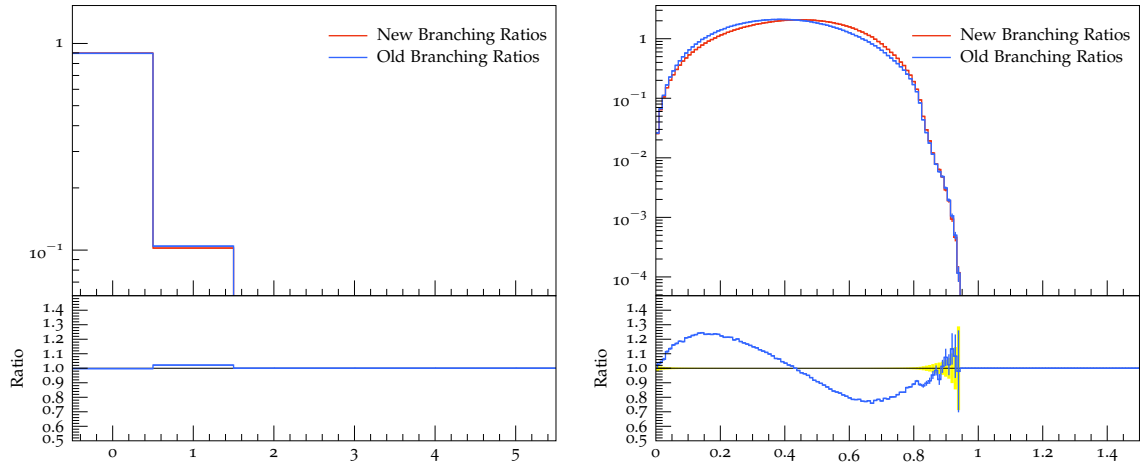
Figure 4.1: multiplicity and energy spectrum of the e^+

branching ratio of the semileptonic decay in a Λ resulting in a nearly equal multiplicity but a significant different energy spectrum for both leptons. The sharp increase at the beginning of the muon energy spectrum comes from the bigger rest mass than the electron. This energy is needed to create a detectable on-shell muon. The two main process to create lepton are the semileptonic decay in Λ and n. Only the branching ratios for the Λ were changed. The higher rest mass of the Λ compared to the neutron lead to an significant energy shift. On the other hand the same number of leptons were created in this process. But compared to the other the branching ratio shifted a little bit to the muon, visible in the plots. The same result for the probability of the multiplicity of the muon proof that the changes in the branching ratios are proportional.

If the plots from the whole decays are considered it becomes clear that these edits also drastically changes the behavior in the final state.

The plots (4.3) from the π^+ show drastic changes. Through the update the probability for
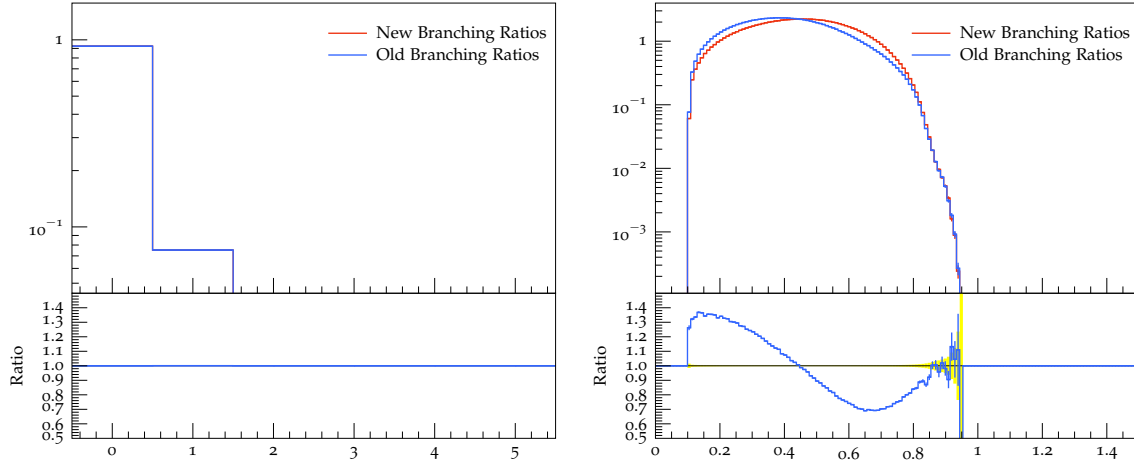
Figure 4.2: multiplicity and energy spectrum of the μ^+
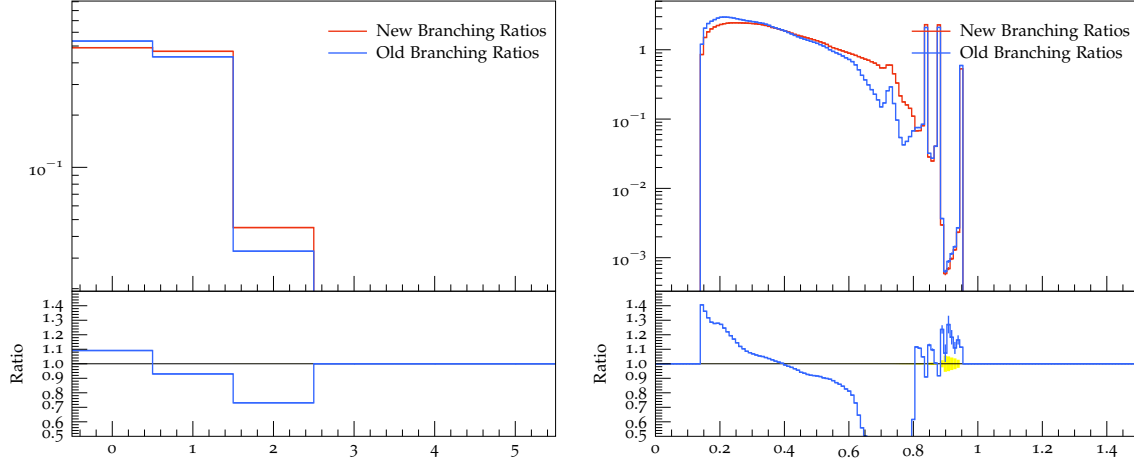
Figure 4.3: multiplicity and energy spectrum of the π^+

no and one particle becomes equal. This leads mainly from the processes with Outgoing part 3224,211,-211 and 3212,211 because there only one π^+ is created and both ratios are increased. The adding of the process with the outgoing part 3112,211,211 is the reason for the increase of 2-multiplicity events. The padding of the gap near 0.7 GeV comes also from a created process, 3122,211,111. The reason for this clear identification can be located in the Plot (4.9) of the π. There the same gap is filled. The last peak is obtained from 2112,211. Only two particles were created and so the the pion get an very high energy. This process is also probable with 0.3%. That's explain the peak. The second peak results from 3122,211 because the Λ has slightly higher mass than the n and so the peak is moved backwards. The peak that is very close to the Λ peak results from the process 3212,211. The Σ has nearly the same mass and so the peaks are very close. The peak with the lowest energy belongs to a decay that doesn't changed and so it is not included in this thesis. The process is $Lambda_c^+ \rightarrow \Delta(1232) + \pi^+$ with an BR of

0.3%. The mass of the $\Delta(1232)$ is higher compared to the others and so the peak has to be at a lower position. The picture (4.9) is very similar to (4.3). In further decays this graph is not
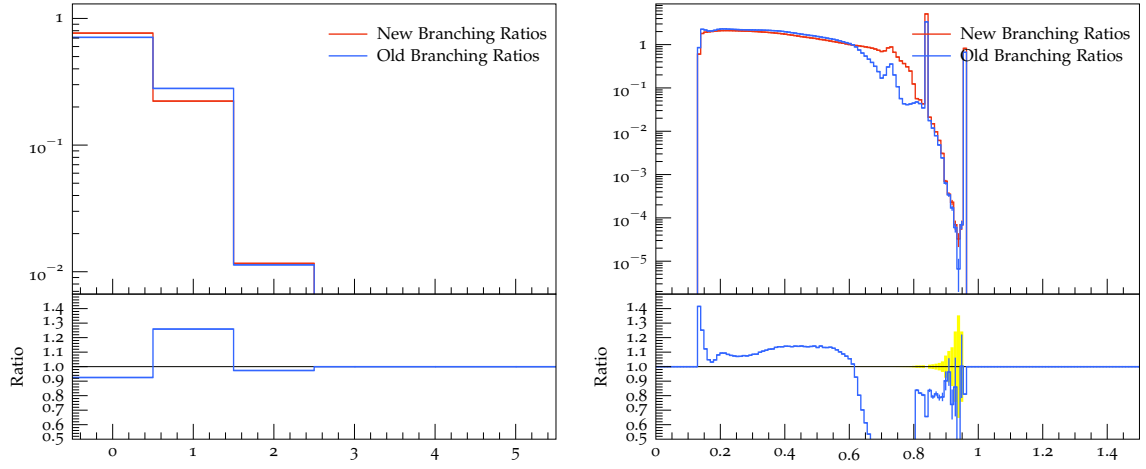
Figure 4.4: multiplicity and energy spectrum of the π

visible because the π is not stable. The peak at the highest energy comes from 2212,111. The peak is nearly on the same position because the mass of the proton is nearly the mass of the neutron. There exists no decay channel in a Λ baryon for the neutral pion. So the pick at this position is missing. The others peak are the same because the mass of the charged baryons only slightly different to the correspondending neutral baryon. The diagram (4.5) show only
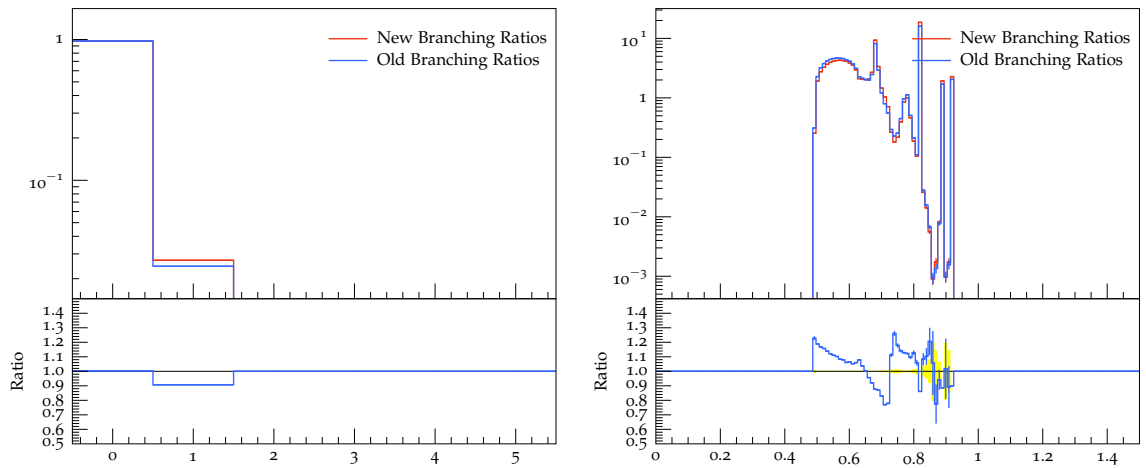
Figure 4.5: multiplicity and energy spectrum of the K^+

little changes. No processes were added and so this resukt is aspected. Through the masses of the other particle in the final state the peaks can be connected to the different processes. From right to the left peaks the decay partner are Λ, Σ, Ξ, $\Sigma(1385)$ and $\Xi(1530)$. The events that are missed in (4.6) are in (4.7) because the process 2212,-311 was changed to 2212,310
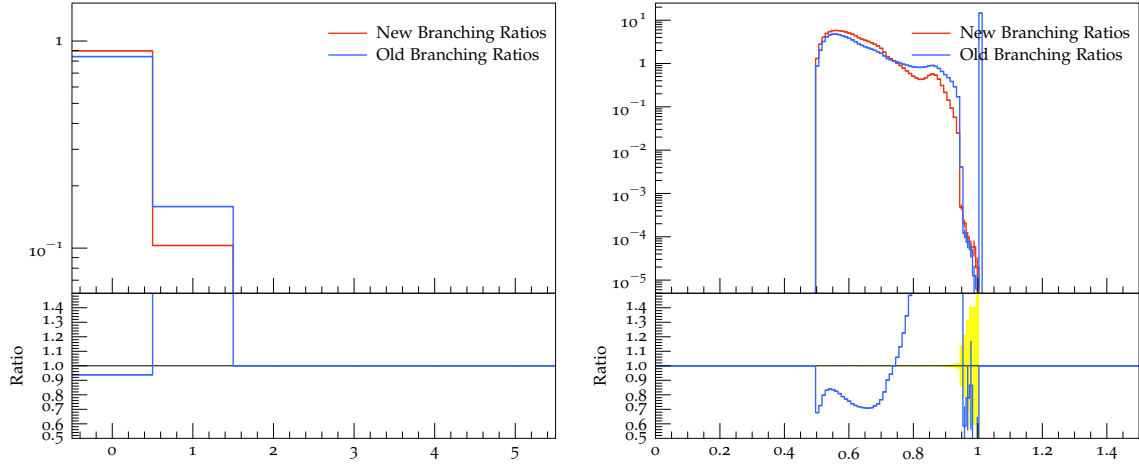
Figure 4.6: multiplicity and energy spectrum of the $\bar{K}$
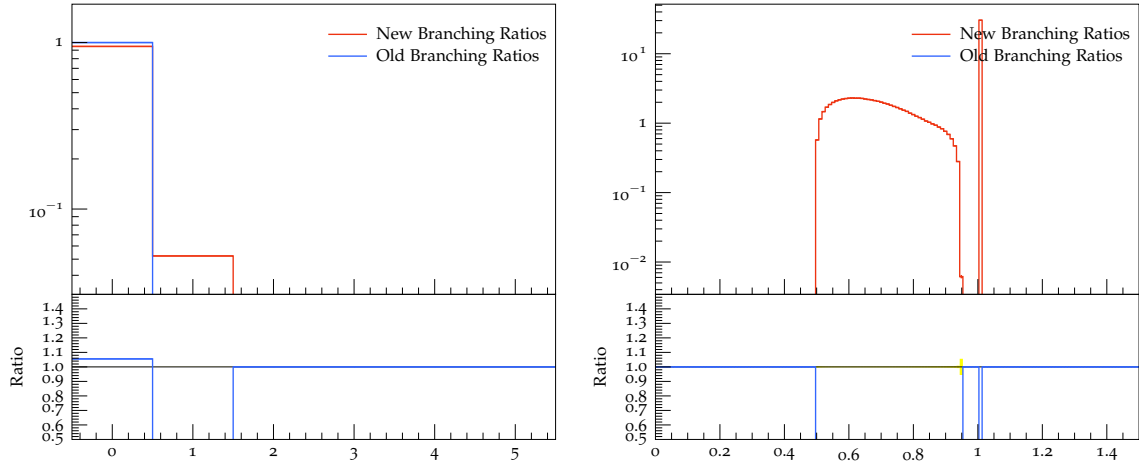
Figure 4.7: multiplicity and energy spectrum of the K_s

and 2212,-311,211,-211 to 2212,310,211,-211. This leads to the two diagrams. The peak in (4.7) belongs to the proton Σ^+ is the reason for the high isolated peak and $\Sigma(1385)+$ for the peak on the hill. The diagrams are changed because the branching ratios were changed, they decreased The decrease of the process 2212,211,211,-211,-211 has an dramatically impact of the multiplicity diagram because it is the only one that produces two π^-. The red bulge is a superposition of all little chances because no processes were changed so drastically.
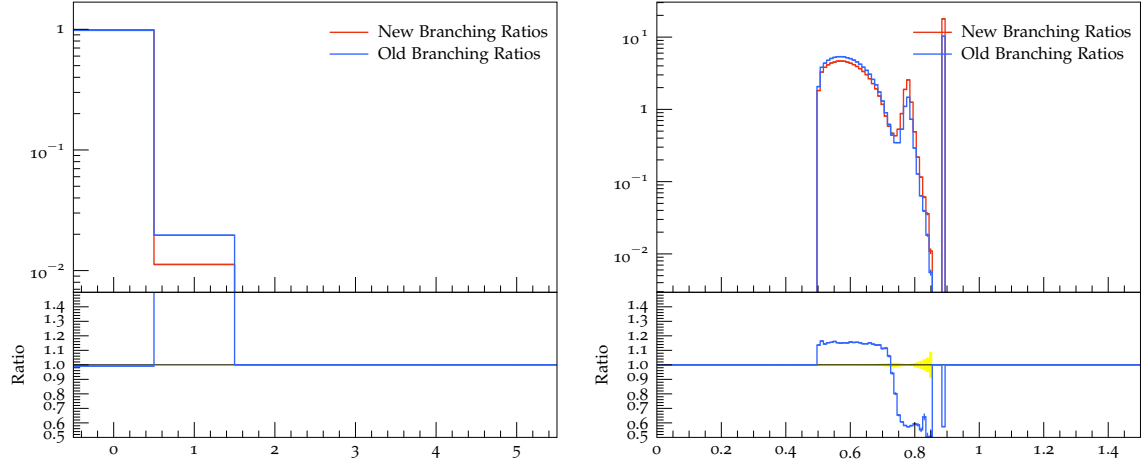
Figure 4.8: multiplicity and energy spectrum of the K
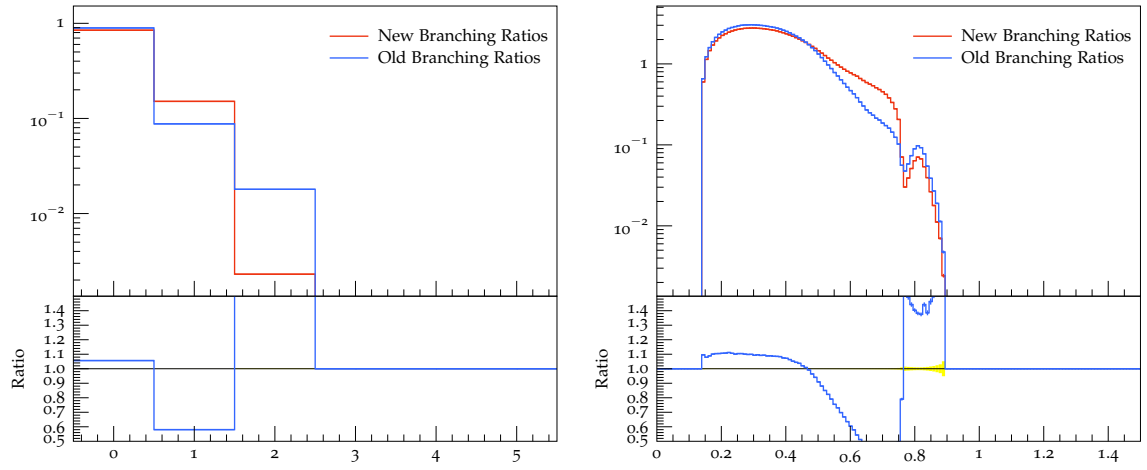
Figure 4.9: multiplicity and energy spectrum of the π^-

4.2 Form Factor Models

All diagrams of the form factors shwo the same behavior. There is no difference in the semileptonic decays in electron or muon except of an sharp increase of the beginnig of the graph for the muon. But this comes from the higher mass of the muon compared to the electron.
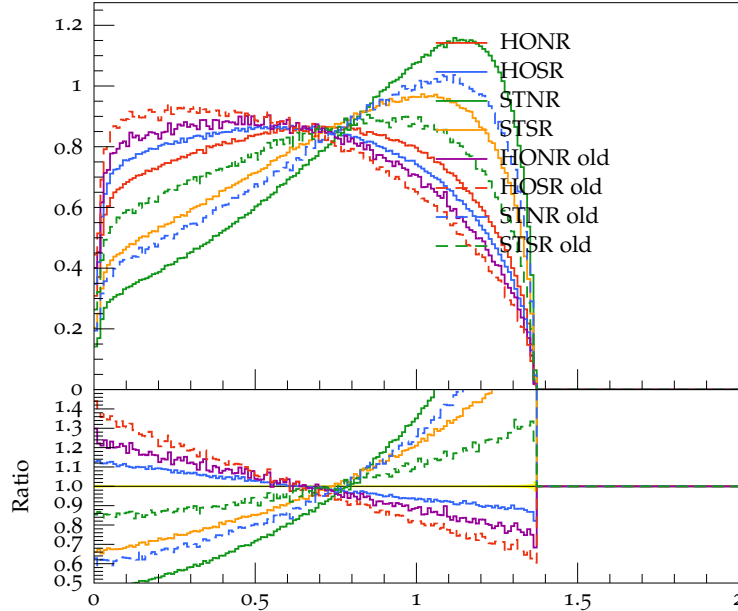
Figure 4.10: Comparison from the already implemented form factor models in leadding order (old) and with all factors for Λ

The diagram (4.10) shows that influence of the higher form factors is for this model not neglectable. So it is important to uncomment the Y function of (3.9) in `VA_B_B.C`. This will be obtain more accurate results because the author of these models make his calculations with all terms and not only with the leading order form factors. The deviations amon themselves are very impressive. The harmonic oszillator ones have general a more falt run in contrast to the sturmian ones with a linear increase an then a sharp decline.

The both parametrization for the light-cone sum rule in (4.11) for different twist show the similar properties. Twist 6 looks like that the steep ascent will increase with a higher twist number but without more calculations with higher twist numbers it is only a theory.

The behavior of the different parametrization (4.12) of the QCD sum rule model is for the two classes of parametrizations very different. The pole parametrizations itself are very similar. They only have little deviations. The general curve is flat and has no small maximum. The complete parametrizations on the other hand have a clear maxmimum and a more steep slope. The full parametrisation with the contiunuums model triangualr and $\kappa = 2$ is an exception. This one describes more the transition between the parametrizations.

The diagram (4.13) shows the big differences between the difference models. The spread
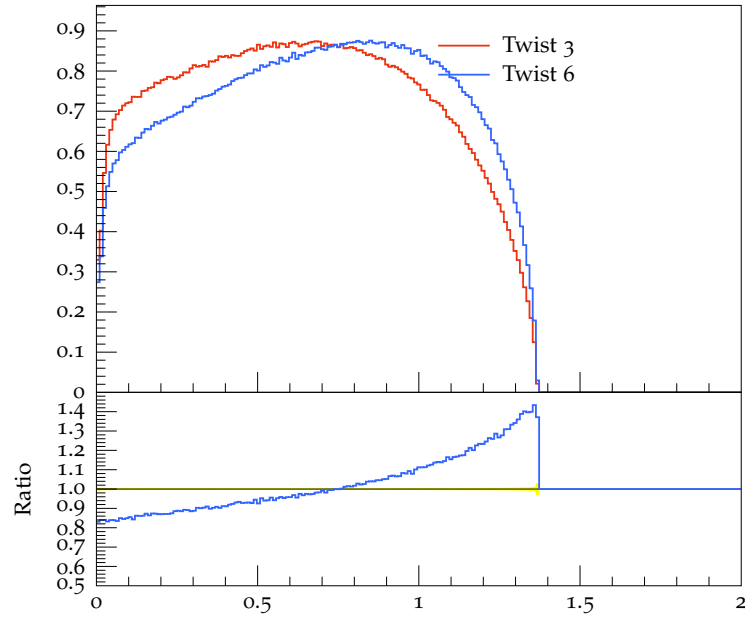
Figure 4.11: Comparison from the different parametrization of the LCSR model for Λ

between the curves is very high and experimental data is needed to really compare this data and select the right form factor model.

The CCQM and the RQM are very similar.

The form factor models (4.14) shows in general a more flat run. Only the CCQM and the RQM have an computation for the neutron. The other models were used with the harmonic oszillator semi relativistic model (HOSR). This model was the previous default. Important to register is that through the lower mass of the neutron the bigger range has to be discribed by the model.

In (4.15) is a comparison with the original implemented form factor models. The LCSR have an analogical like the HONR.

This (4.16) is a comparison of all four form factor models for the neutron because for LCSR and STSR the HOSR is used. The models for the neutron didn't have such big deviations like the ones for the Λ. So the choice of the model is for the neutron not so important because all of this will give similar results.

And so the concentration should lay on the Λ. But without good experimental datas a clean comparison is not possible and so no model can be preferred.
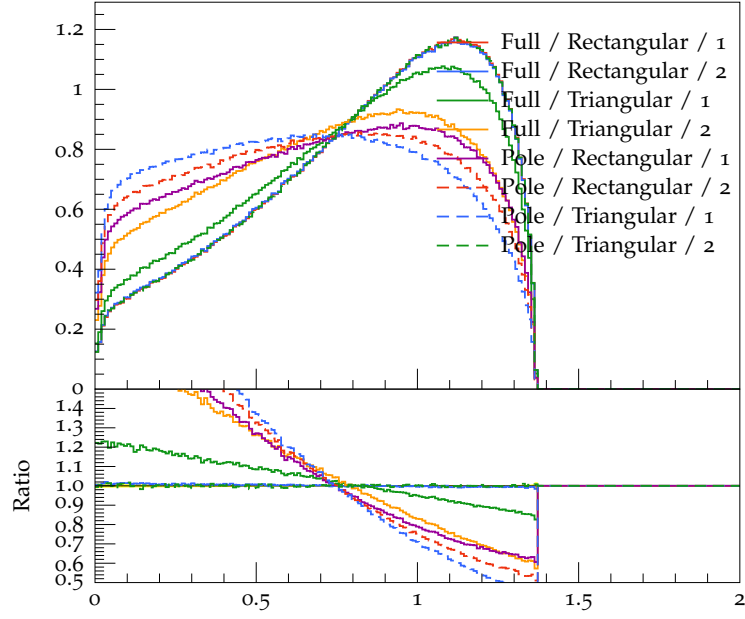
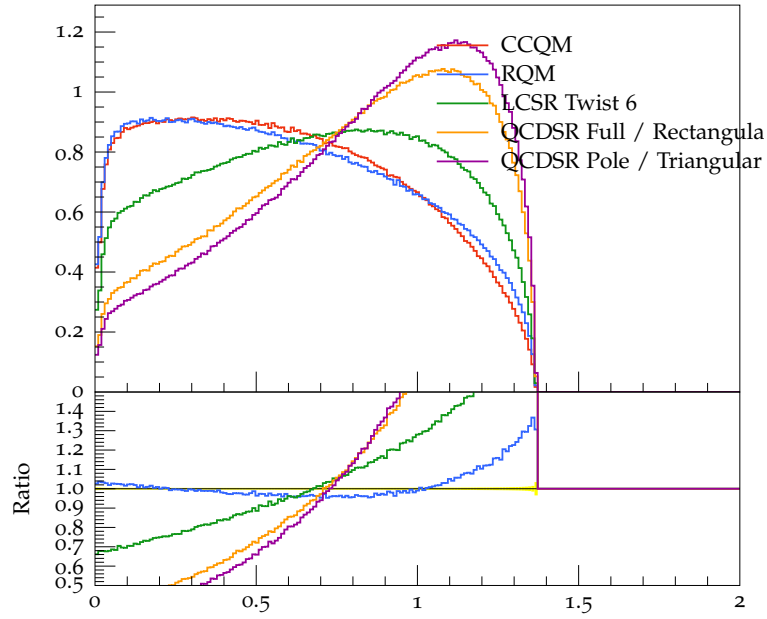**Figure 4.12:** Comparison from the different parametrization of the QCDSR model for Λ

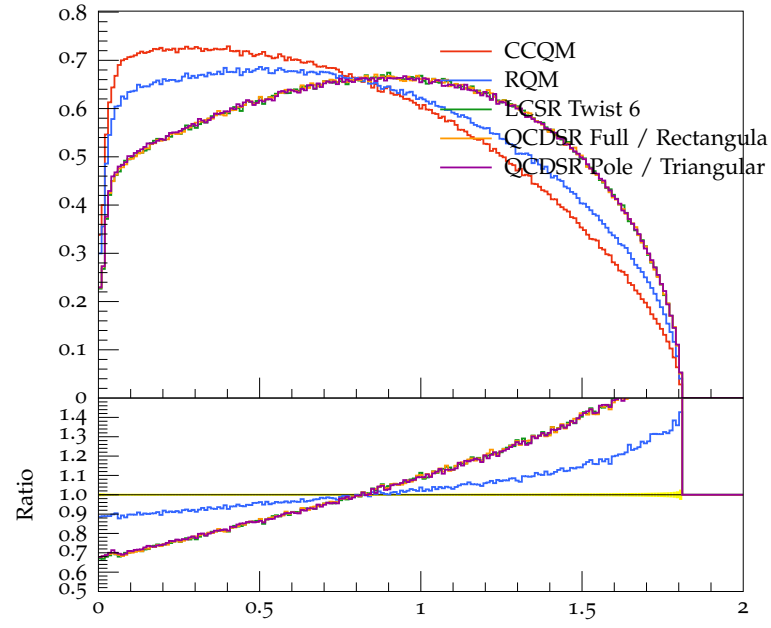**Figure 4.13:** Comparison from some of the self implemented form factor models for Λ

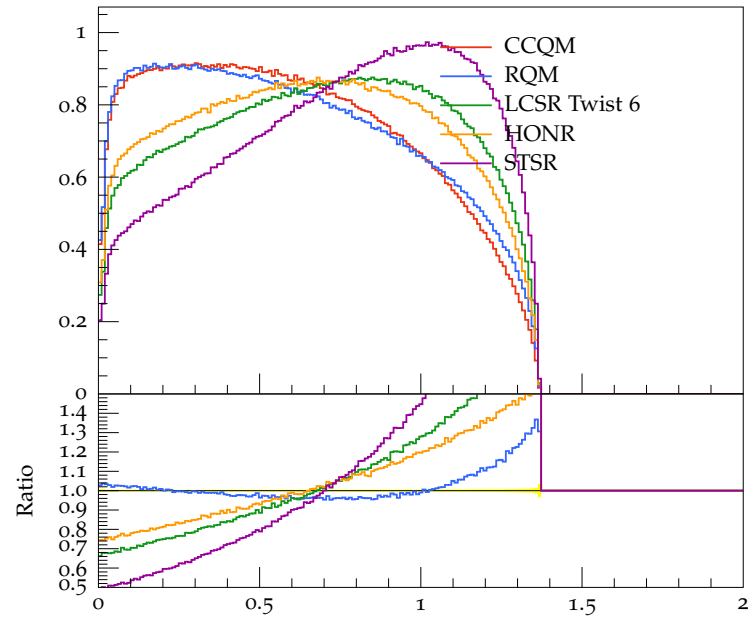**Figure 4.14:** Comparison from some of the self implemented form factor models for the neutron

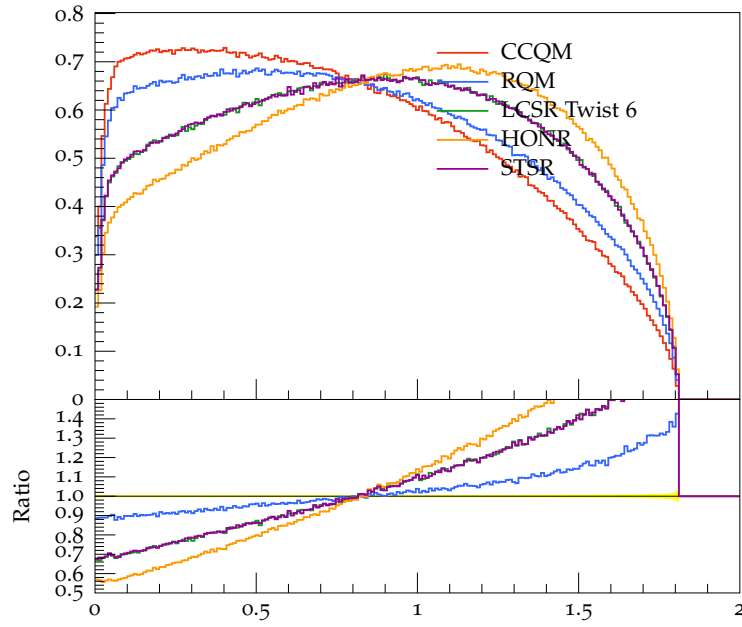**Figure 4.15:** Comparison from the already implemented form factor models with some of the self implemented ones for Λ

Figure 4.16: Comparison from the already implemented form factor models with some of the self implemented ones for the neutron

5 Summary and Outlook

This bachelor thesis gave a little contribution to world biggest epxeriment through the update of the branching ratios of the Λ_c^+. Every Baryon is important because with everyone the modeling of the processess in the nature becomes more accurate. Through more exact modeling the comparison between our laws of nature, in this special case the standard model of particle physics, and the reallity becomes better and better again. So discrepancies are discoverable and the theory can be improved.

This work shows that the position of th peaks in the energy spectrum are correlated to the masses of the other particles in the final state. These peaks occurs only with two particles in the final state. This comes from the determination of the four-momentum in this case. The particle have no other choice to put the momentum elsewhere.

There exists a lot of different form factor models and the behavior of them can partially very different, flat or steep run, only a comparison with experimental data can clarify. This leads to a lot of measurements because every particle have a slightly different behavior when its decays. But only with these amount of data a clear answer for every particle is possible.

The non relativistic quak model [9] was introduced am implement with this thesis in `Sherpa`. For the exicted Λ states didn't exist so much experimental data. The concentration has layed on the other models because it would be easier to get data. But as a continuation to this work this model can be tested. Further an implementation of the form factor model from Lattice QCD [10] would be a great work. The Lattice QCD is a modern method of the QCD and used in many aspect.

6 Bibliography

[1] R. S. Marques de Carvalho et al. "Form factors and decay rates for heavy Λ semileptonic decays from QCD sum rules". In: *Phys. Rev. D* 60 (3 1999), p. 034009. DOI: 10.1103/PhysRevD.60.034009. URL: https://link.aps.org/doi/10.1103/PhysRevD.60.034009.

[2] A. Ceccucci (CERN), Z. Ligeti (LBNL), and Y. Sakai (KEK). *THE CKM QUARK-MIXING MATRIX*. 2016. URL: http://pdg.lbl.gov/2016/reviews/rpp2016-rev-ckm-matrix.pdf (visited on 03/27/2017).

[3] C. Patrignani et al.(Particle Data Group). *CHARMED BARYONS* Λ_c^+. 2016. URL: http://pdglive.lbl.gov/Particle.action?node=S033&init= (visited on 03/09/2017).

[4] R. N. Faustov and V. O. Galkin. "Semileptonic decays of Λ_b baryons in the relativistic quark model". In: *Phys. Rev. D* 94 (7 2016), p. 073008. DOI: 10.1103/PhysRevD.94.073008. URL: https://link.aps.org/doi/10.1103/PhysRevD.94.073008.

[5] R. N. Faustov and V. O. Galkin. "Semileptonic decays of Λ_c baryons in the relativistic quark model". In: *Eur. Phys. J.* C76.11 (2016), p. 628. DOI: 10.1140/epjc/s10052-016-4492-z. arXiv: 1610.00957 [hep-ph].

[6] Thomas Gutsche et al. "Heavy-to-light semileptonic decays of Λ_b and Λ_c baryons in the covariant confined quark model". In: *Phys. Rev.* D90.11 (2014). [Erratum: Phys. Rev.D94,no.5,059902(2016)], p. 114033. DOI: 10.1103/PhysRevD.90.114033,10.1103/PhysRevD.94.059902. arXiv: 1410.6043 [hep-ph].

[7] Thomas Gutsche et al. "Semileptonic decays $\Lambda_c^+ \to \Lambda \ell^+ \nu_\ell$ ($\ell = e, \mu$) in the covariant quark model and comparison with the new absolute branching fraction measurements of Belle and BESIII". In: *Phys. Rev.* D93.3 (2016), p. 034008. DOI: 10.1103/PhysRevD.93.034008. arXiv: 1512.02168 [hep-ph].

[8] Ming-Qiu Huang and Dao-Wei Wang. "Semileptonic decay Lambda(c) —> Lambda l+ nu from QCD light-cone sum rules". In: (2006). arXiv: hep-ph/0608170 [hep-ph].

[9] Md Mozammel Hussain and Winston Roberts. "Λ_c Semileptonic Decays in a Quark Model". In: *Phys. Rev.* D95.5 (2017). [Addendum: Phys. Rev.D95,no.9,099901(2017)], p. 053005. DOI: 10.1103/PhysRevD.95.099901,10.1103/PhysRevD.95.053005. arXiv: 1701.03876 [nucl-th].

[10]   Stefan Meinel. "$\Lambda_c \to \Lambda l^+ \nu_l$". In: *Phys. Rev. Lett.* 118 (8 2017), p. 082001. DOI: `10.1103/`
       `PhysRevLett.118.082001`. URL: `https://link.aps.org/doi/10.1103/PhysRevLett.`
       `118.082001`.

[11]   Muslema Pervin, Winston Roberts, and Simon Capstick. "Semileptonic decays of heavy
       lambda baryons in a quark model". In: *Phys. Rev.* C72 (2005), p. 035201. DOI: `10.1103/`
       `PhysRevC.72.035201`. arXiv: `nucl-th/0503030` `[nucl-th]`.

[12]   Frank Siegert. "Simulation of hadron decays in SHERPA". In: (2007).

A Appendix

A.1 Decays.dat

Table A.1: Full list of changes in the Decays.dat from the Λ_c^+

Status	Outgoing Part.	BR(Delta BR)[Origin]	Decay
		Modes with nucleons/Deltas	
old	2212,-311	0.023(0.006)[PDG]	$\Lambda_c^+ \to P^+ + K_b$
new	2212,310	0.0158(0.0008)[PDG]	$\Lambda_c^+ \to P^+ + K_s$
old	2212,-313	0.016(0.005)[PDG]	$\Lambda_c^+ \to P^+ + K^*(892)_b$
new	2212,-313	0.0198(0.0028)[PDG]	
old	2212,-321,211	0.028(0.008)[PDG]	$\Lambda_c^+ \to P^+ + K^- + \pi^+$
new	2212,-321,211	0.035(0.004)[PDG]	
old	2212,-311,111	0.033(0.010)[PDG]	$\Lambda_c^+ \to P^+ + K_b + \pi$
new	2212,310,111	0.0199(0.0013)[PDG]	
old	2212,-311,221	0.012(0.004)[PDG]	$\Lambda_c^+ \to P^+ K_b + \eta$
new	2212,-311,221	0.016(0.004)[PDG]	
old	2212,-311,211,-211	0.026(0.007)[PDG]	$\Lambda_c^+ \to P^+ + K_b + \pi^+ + \pi^-$
new	2212,-311,211,-211	0.049(0.004)[PDG]	
old	2212,-311,211,-211	0.026(0.007)[PDG]	$\Lambda_c^+ \to P^+ + K_b + \pi^+ + \pi^-$
new	2212,310,211,-211	0.0166(0.0012)[PDG]	$\Lambda_c^+ \to P^+ + K_s + \pi^+ + \pi^-$
old	2212,-323,211	0.016(0.005)[PDG]	$\Lambda_c^+ \to P^+ + K^*(892)_b^+ + \pi^+$
new	2212,-323,211	0.015(0.005)[PDG]	
old	2212,-321,211,111	0.036(0.012)[PDG]	$\Lambda_c^+ \to P^+ + K^- + \pi^+ + \pi$
new	2212,-321,211,111	0.046(0.09)[PDG]	
old	2212,-321,211,211,-211	0.0011(0.0008)[PDG]	$\Lambda_c^+ \to P^+ + K^- + \pi^+ + \pi^+ + \pi^-$
new	2212,-321,211,211,-211	0.0014(0.001)[PDG]	
old	2212,-321,211,111,111	0.008(0.004)[PDG]	$\Lambda_c^+ \to P^+ + K^- + \pi^+ + \pi + \pi$
new	2212,-321,211,111,111	0.01(0.005)[PDG]	
old	2212,333	0.00082(0.00027)[PDG]	$\Lambda_c^+ \to P^+ + \phi(1020)$
new	2212,333	0.00104(0.00021)[PDG]	

S = 0			
old	2212,321,-321	0.00035(0.00017)[PDG]	$\Lambda_c^+ \rightarrow P^+ + K^+ + K^-$
new	2212,321,-321	0.00044(0.00018)[PDG]	
S = 0			
old	2212,211,211,-211,-211	0.018(0.012)[PDG]	$\Lambda_c^+ \rightarrow P^+ + \pi^+ + \pi^+ + \pi^- + \pi^-$
new	2212,211,211,-211,-211	0.0023(0.0015)[PDG]	
S = 0			
old	2212,9010221	0.0028(0.0019)[PDG]	$\Lambda_c^+ \rightarrow P^+ + f(0980)$
new	2212,9010221	0.0035(0.0023)[PDG]	
S = 0			
deleted	2212,211,-211	0.0007(0.0007)[PDG]	$\Lambda_c^+ \rightarrow P^+ + \pi^+ + \pi^-$
S = 0			
old	2224,-321	0.0086(0.003[PDG]	$\Lambda_c^+ \rightarrow \Delta(1232)^{++} + K^-$
new	2224,-321	0.0109(0.0025)[PDG]	
Modes with hyperons			
old	3122,211	0.0107(0.0028)[PDG]	$\Lambda_c^+ \rightarrow \Lambda + \pi^+$
new	3122,211	0.0130(0.0007)[PDG]	
created	3122,211,111	0.071(0.0004)[PDG]	$\Lambda_c^+ \rightarrow \Lambda + \pi^+ + \pi$
created	3122,213	0.036(0.013)[PDG]	$\Lambda_c^+ \rightarrow \Lambda + \rho(770)^+$
S = 0			
old	3122,321	0.0005(0.00016)[PDG]	$\Lambda_c^+ \rightarrow \Lambda + K^+$
new	3122,321	0.00061(0.00012)[PDG]	
old	3122,211,113	0.011(0.005)[PDG]	$\Lambda_c^+ \rightarrow \Lambda + \pi^+ + \rho(770)$
new	3122,211,113	0.015(0.006)[PDG]	
old	3122,221,211	0.018(0.006)[PDG]	$\Lambda_c^+ \rightarrow \Lambda + \eta + \pi^+$
new	3122,221,211	0.022(0.005)[PDG]	
old	3122,223,211	0.018(0.006)[PDG]	$\Lambda_c^+ \rightarrow \Lambda + \omega(782) + \pi^+$
new	3122,223,211	0.015(0.005)[PDG]	
old	3122,321,-311	0.0047(0.0015)[PDG]	$\Lambda_c^+ \rightarrow \Lambda + K^+ + K_b$
new	3122,321,-311	0.0057(0.0011)[PDG]	
old	3114,211,211	0.0055(0.0017)[PDG]	$\Lambda_c^+ \rightarrow \Sigma(1385)^- + \pi^+ + \pi^+$
new	3114,211,211	0.0090(0.0018)[PDG]	
created	3112,211,211	0.021(0.004)[PDG]	$\Lambda_c^+ \rightarrow \Sigma^- + \pi^+ + \pi^+$
old	3212,211	0.0105(0.0028)[PDG]	$\Lambda_c^+ \rightarrow \Sigma + \pi^+$
new	3212,211	0.0129(0.0007)[PDG]	
S = 0			

old	3212,321	0.00042(0.00013)[PDG]	$\Lambda_c^+ \to \Sigma + K^+$
new	3212,321	0.00052(0.00008)[PDG]	
old	3212,211,211,-211	0.0083(0.0031)[PDG]	$\Lambda_c^+ \to \Sigma + \pi^+ + \pi^+ + \pi^-$
new	3212,211,211,-211	0.0113(0.0029)[PDG]	
old	3222,111	0.0100(0.0034)[PDG]	$\Lambda_c^+ \to \Sigma^+ + \pi$
new	3222,111	0.0124(0.001)[PDG]	
old	3222,221	0.0055(0.0023)[PDG]	$\Lambda_c^+ \to \Sigma^+ + \eta$
new	3222,221	0.0070(0.0023)[PDG]	
old	3222,211,-211	0.013(0.005)[PDG]	$\Lambda_c^+ \to \Sigma^+ + \pi^+ + \pi^-$
new	3222,211,-211	0.0457(0.0029)[PDG]	
S = 0			
old	3222,313	0.002[EvtGen]	$\Lambda_c^+ \to \Sigma^+ + K^*(892)$
new	3222,313	0.0036(0.001)[PDG]	
old	3222,223	0.027(0.01)[PDG]	$\Lambda_c^+ \to \Sigma^+ + \omega(782)$
new	3222,223	0.0174(0.0021)[PDG]	
old	3222,333	0.0031(0.0009)[PDG]	$\Lambda_c^+ \to \Sigma^+ + \phi(1020)$
new	3222,333	0.0040(0.0006)[PDG]	
old	3224,113	0.0037(0.0031)[PDG]	$\Lambda_c^+ \to \Sigma(1385)^+ + \rho(770)$
new	3224,113	0.0072(0.0046)[PDG]	
old	3224,221	0.0085(0.0033)[PDG]	$\Lambda_c^+ \to \Sigma(1385)^+ + \eta$
new	3224,221	0.00124(0.00037)[PDG]	
old	3224,211,-211	0.007(0.004)[PDG]	$\Lambda_c^+ \to \Sigma(1385)^+ + \pi^+ + \pi^-$
new	3224,211,-211	0.011(0.006)[PDG]	
old	3322,321	0.0039(0.0014)[PDG]	$\Lambda_c^+ \to \Xi + K^+$
new	3322,321	0.0050(0.0012)[PDG]	
old	3312,321,211	0.0025(0.001)[PDG]	$\Lambda_c^+ \to \Xi^- + K^+ + \pi^+$
new	3312,321,211	0.0062(0.0006)[PDG]	
old	3324,321	0.0026(0.001)[PDG]	$\Lambda_c^+ \to \Xi(1530) + K^+$
new	3324,321	0.0033(0.0009)[PDG]	
semileptonic modes			
old	3122,12,-11	0.021(0.006)[PDG]	$\Lambda_c^+ \to \Lambda + \nu_e + e^+$
new	3122,12,-11	0.036(0.004)[PDG]	
old	3122,14,-13	0.020(0.007)[PDG]	$\Lambda_c^+ \to \Lambda + \nu_\mu + \mu^+$
new	3122,14,-13	0.036(0.004)[PDG]	

A.2 Primary Decays
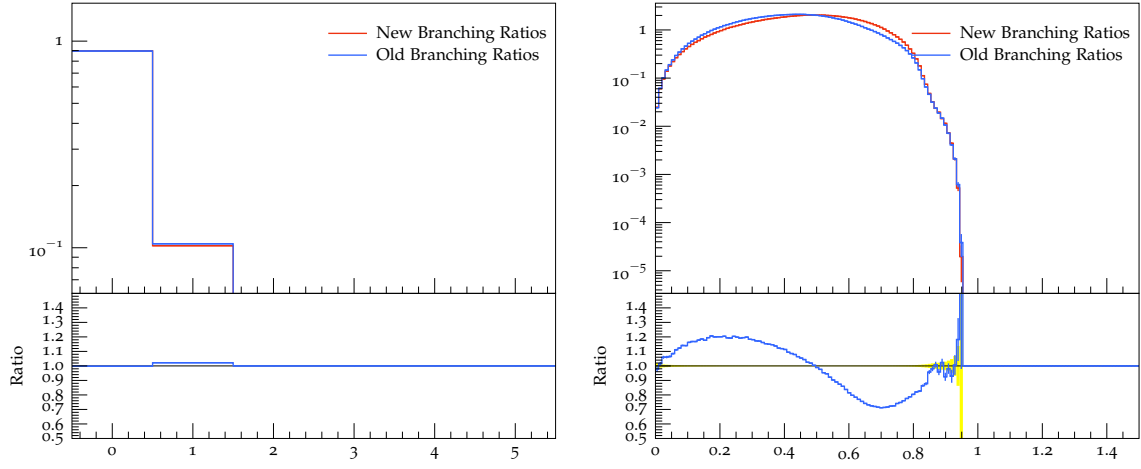
Figure A.1: multiplicity and energy spectrum of the ν_e
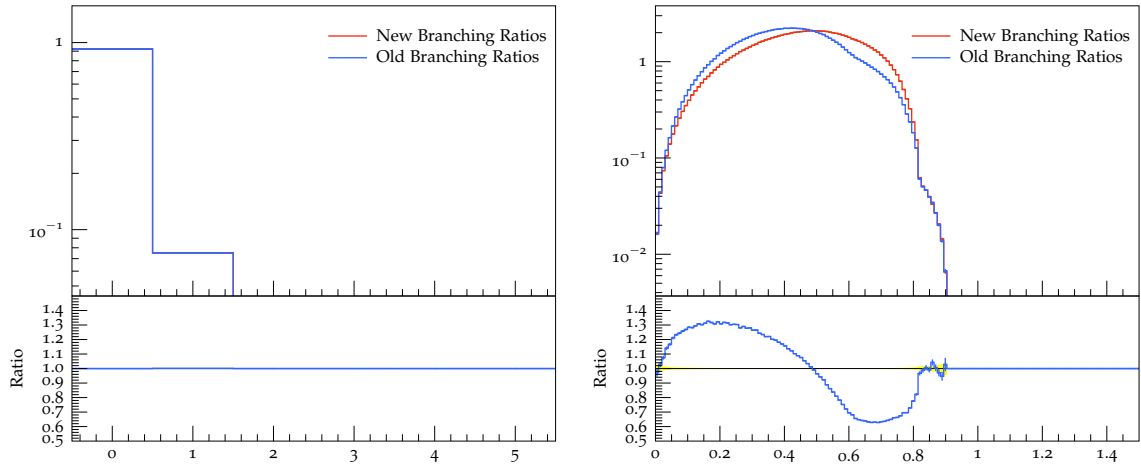
Figure A.2: multiplicity and energy spectrum of the ν_μ
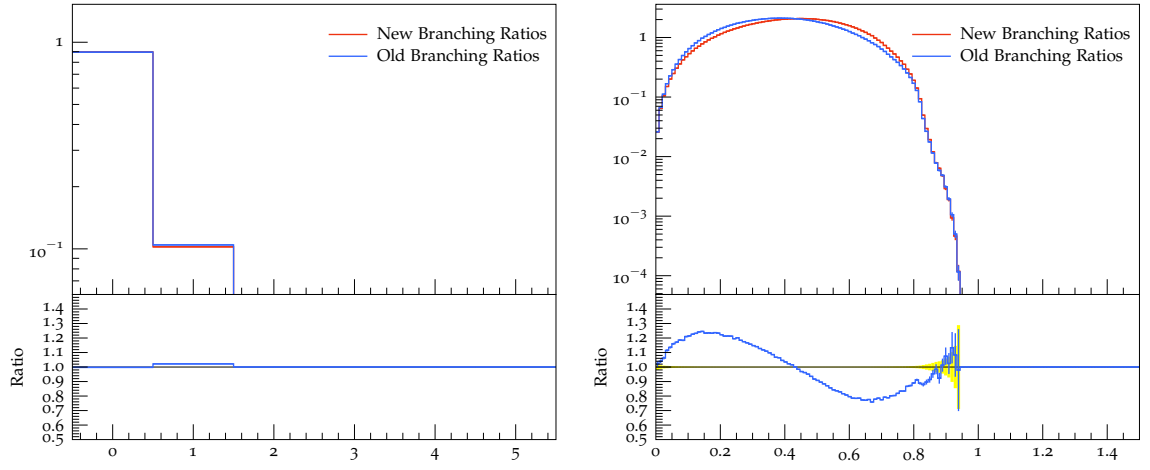
Figure A.3: multiplicity and energy spectrum of the e^+
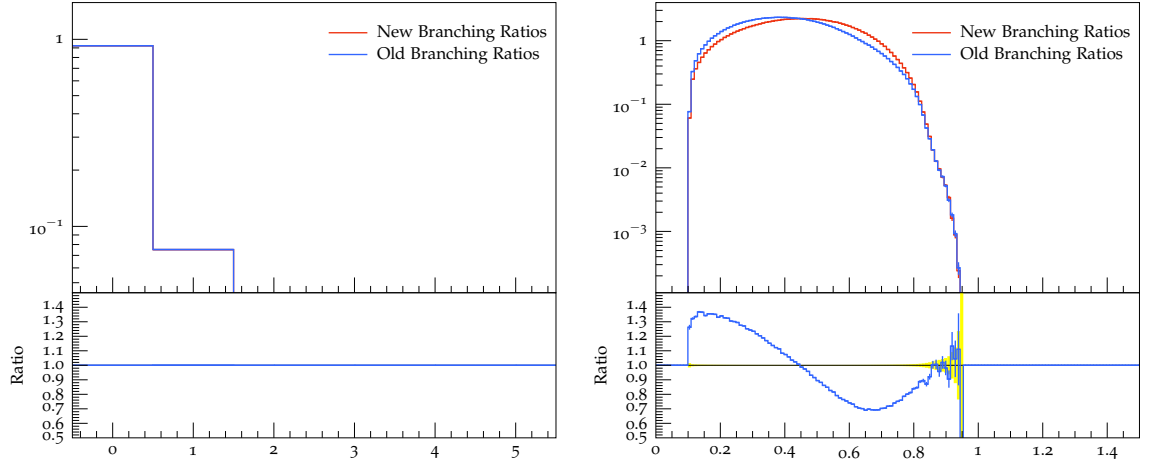
Figure A.4: multiplicity and energy spectrum of the μ^+
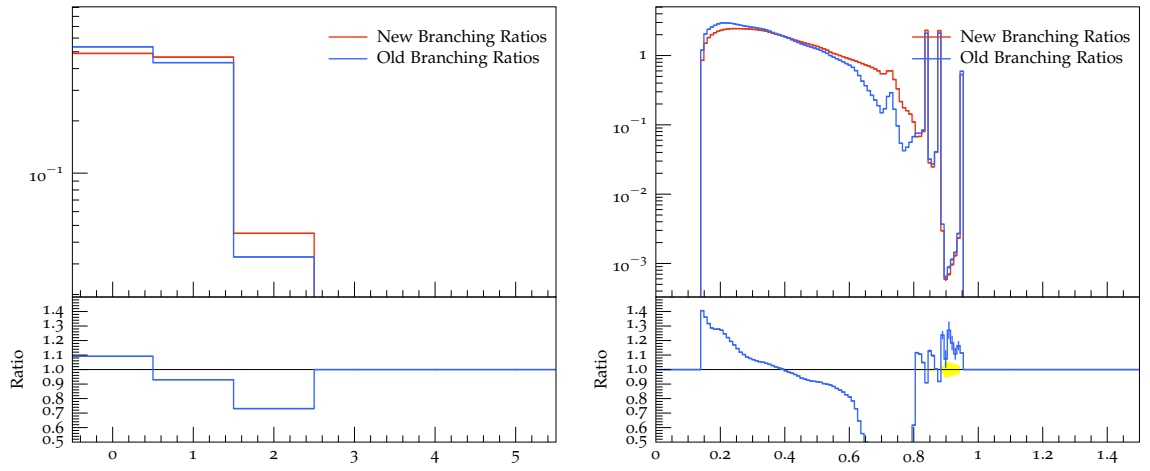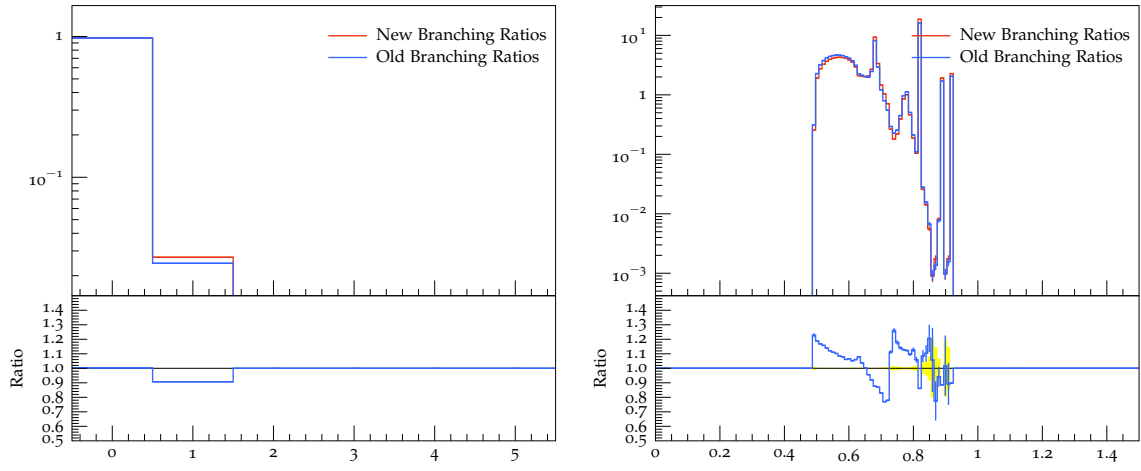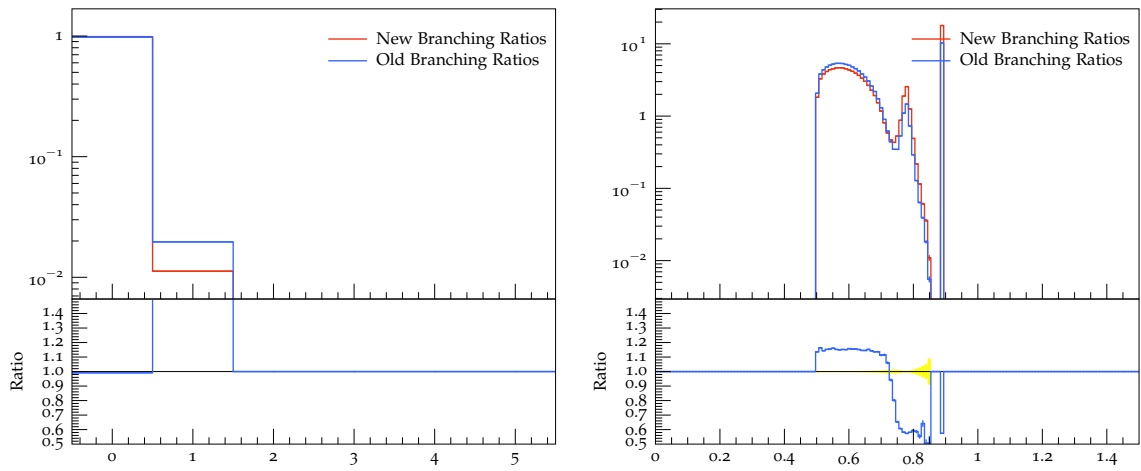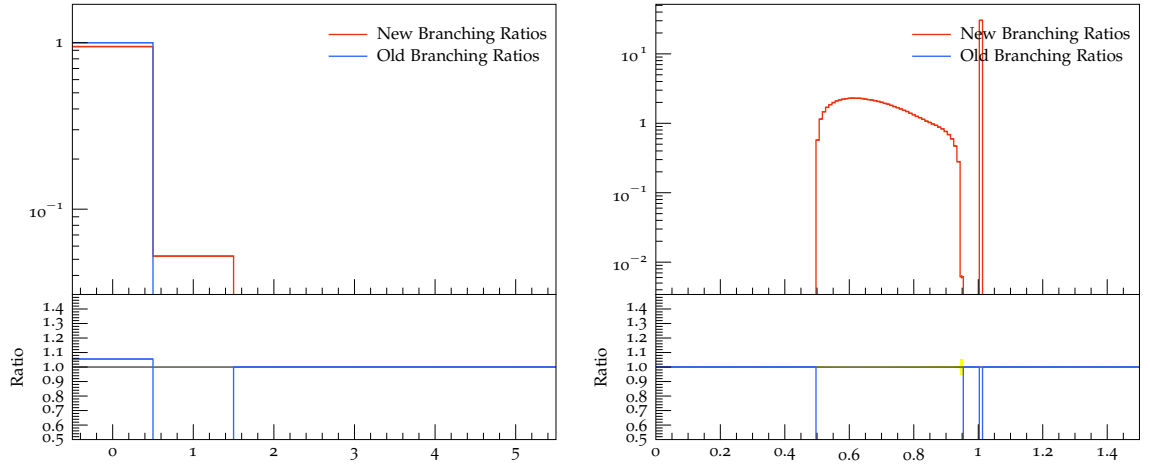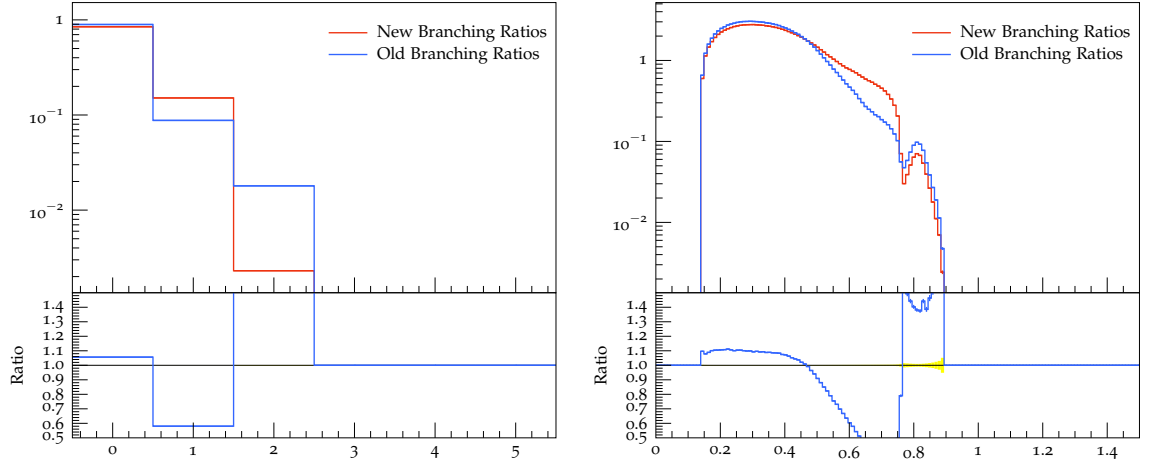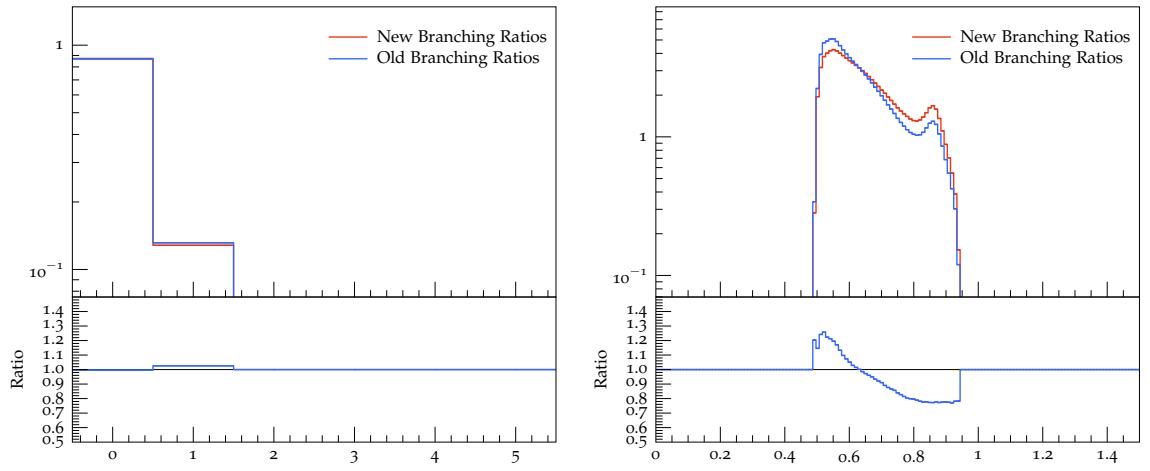

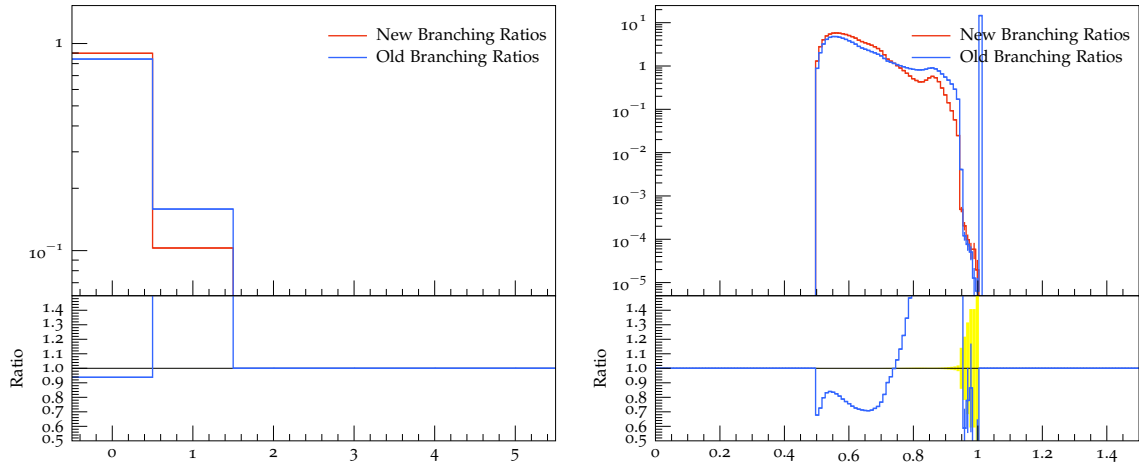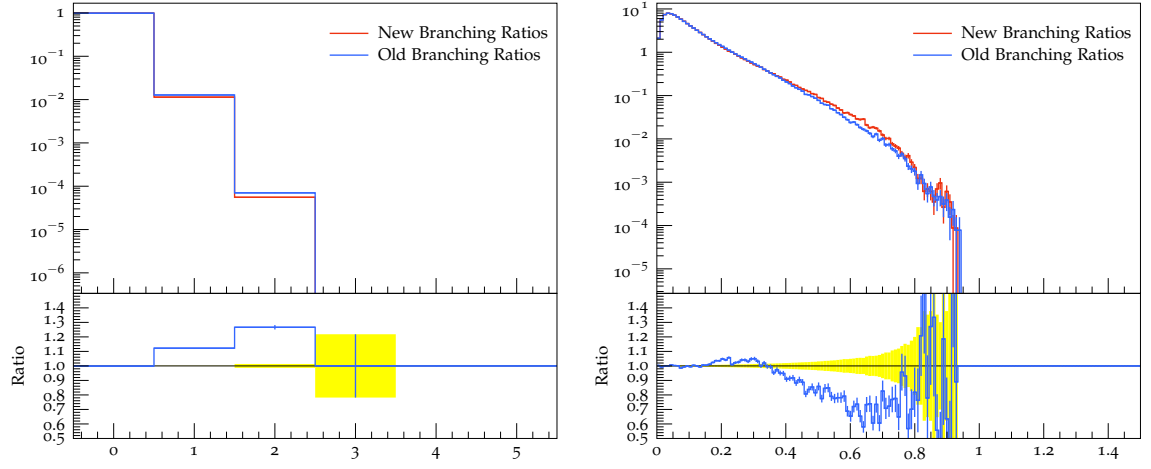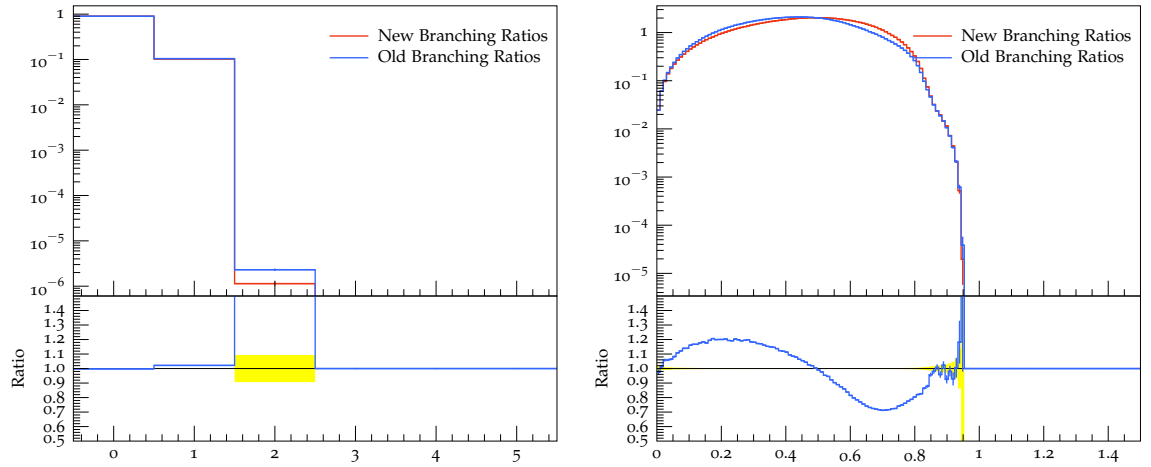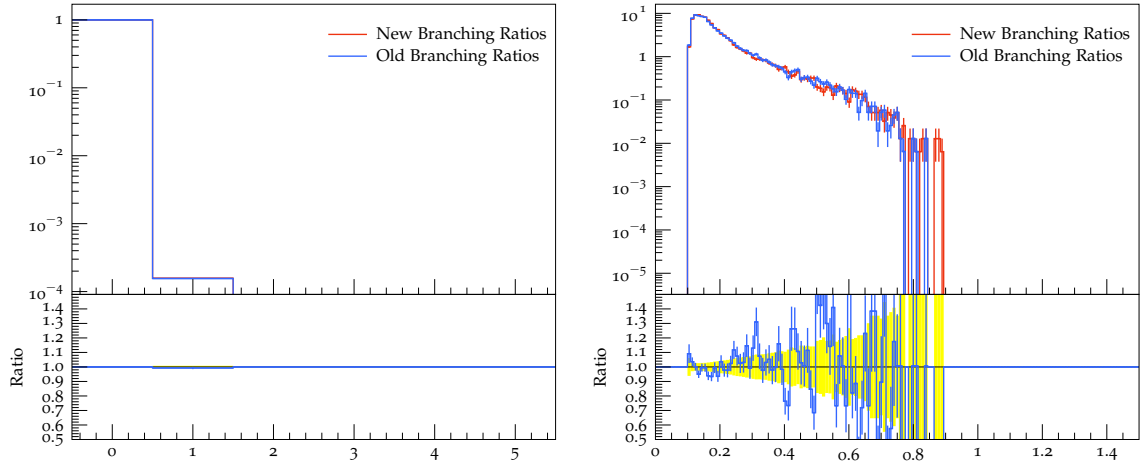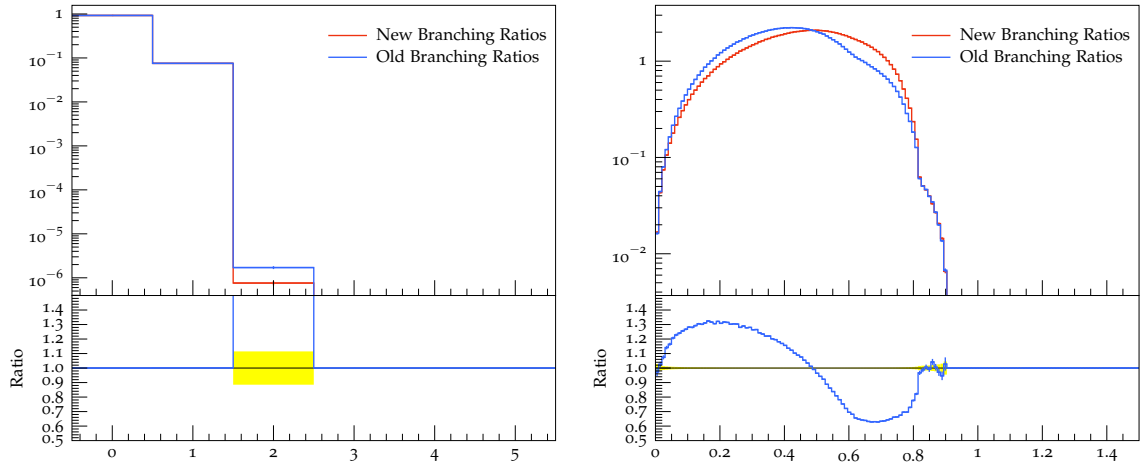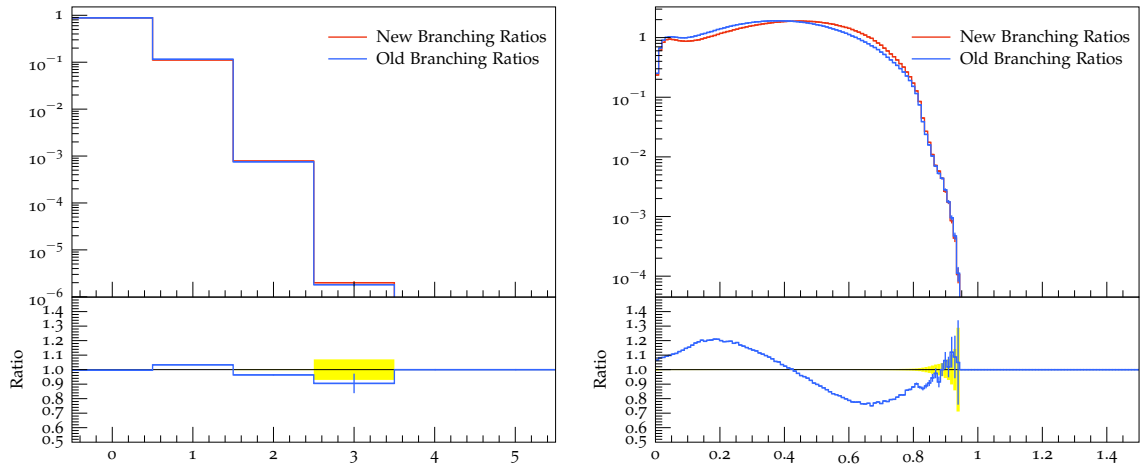**Figure A.5:** multiplicity and energy spectrum of the π^+
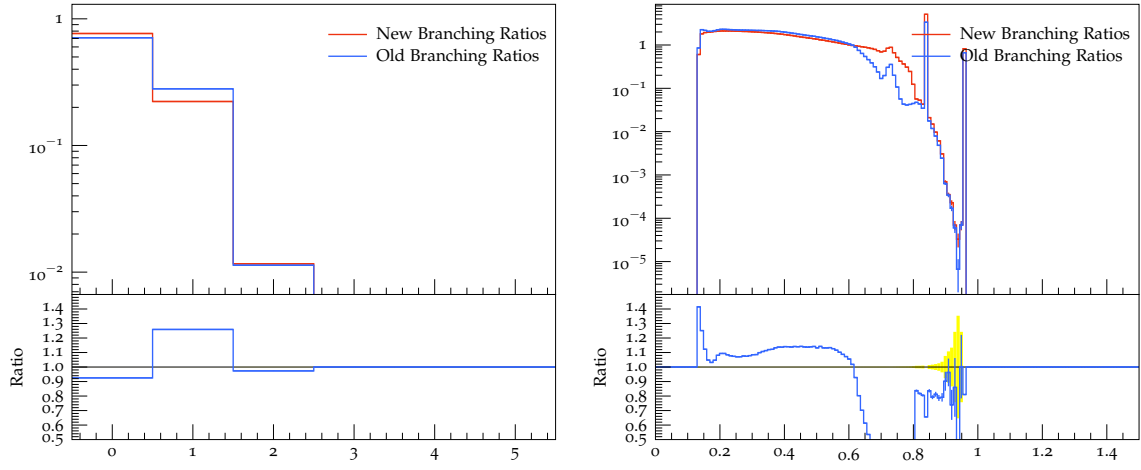
Figure A.6: multiplicity and energy spectrum of the π

Figure A.7: multiplicity and energy spectrum of the K^+

Figure A.8: multiplicity and energy spectrum of the K

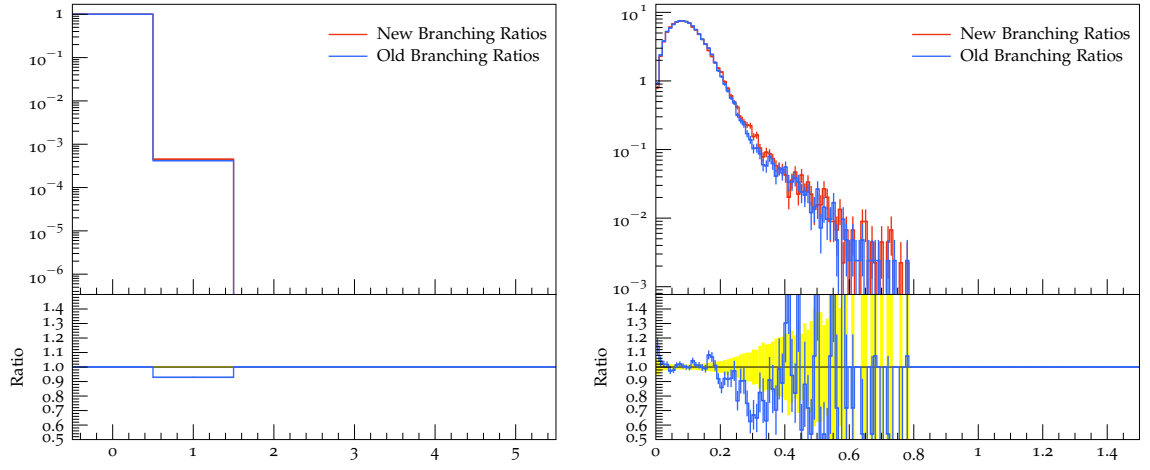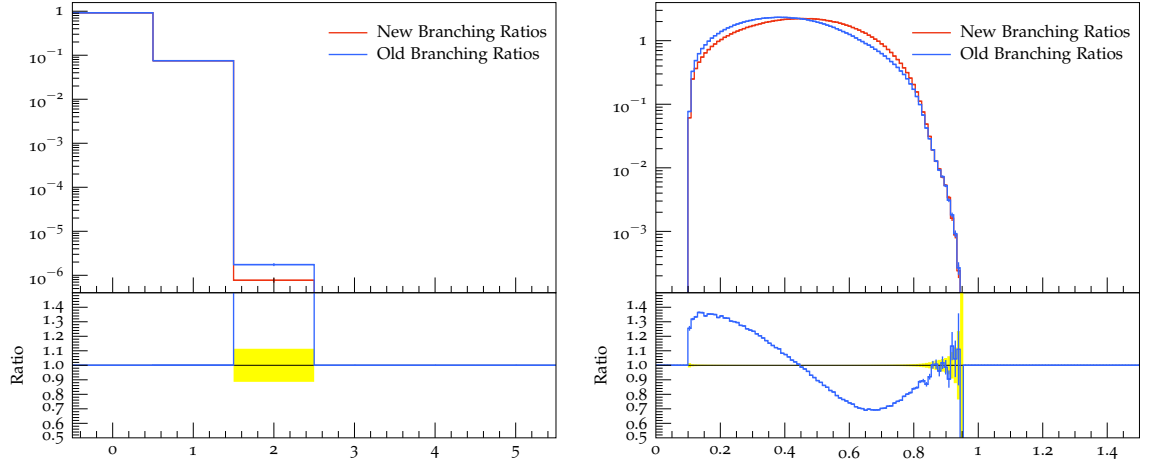**Figure A.9:** multiplicity and energy spectrum of the K_s

Figure A.10: multiplicity and energy spectrum of the π^-

Figure A.11: multiplicity and energy spectrum of the K^-

Figure A.12: multiplicity and energy spectrum of the $\bar{K}$
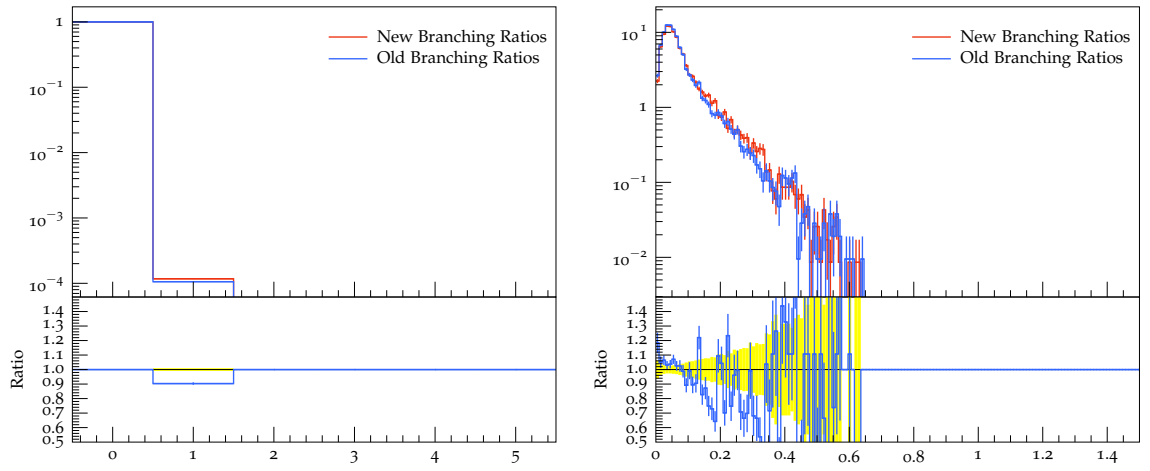
A.3 Complete Decays

Figure A.13: multiplicity and energy spectrum of the e^-

Figure A.14: multiplicity and energy spectrum of the ν_e^-

Figure A.15: multiplicity and energy spectrum of the μ^-

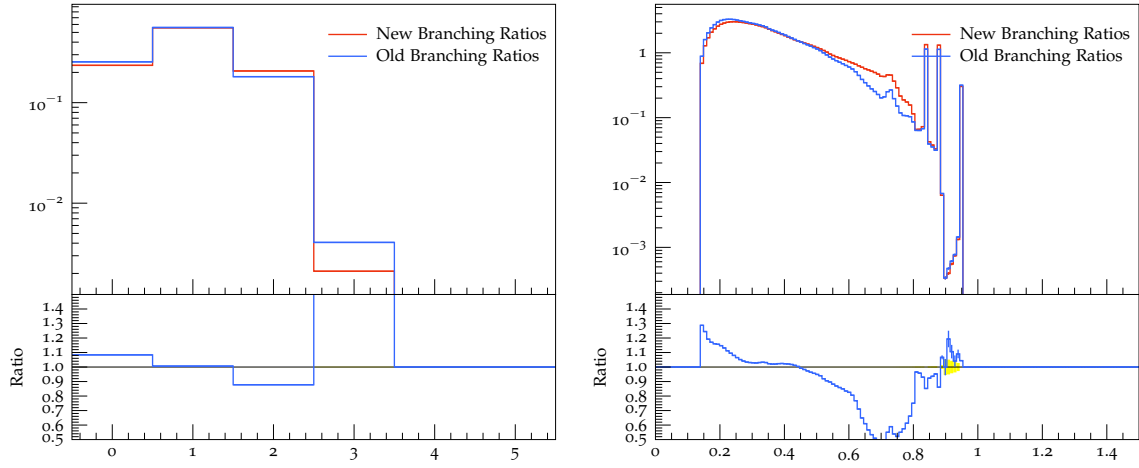**Figure A.16:** multiplicity and energy spectrum of the ν_μ^-

Figure A.17: multiplicity and energy spectrum of the e^+

Figure A.18: multiplicity and energy spectrum of the $\bar{\nu}_e$

Figure A.19: multiplicity and energy spectrum of the μ^+

Figure A.20: multiplicity and energy spectrum of the $\bar{\nu}_\mu$
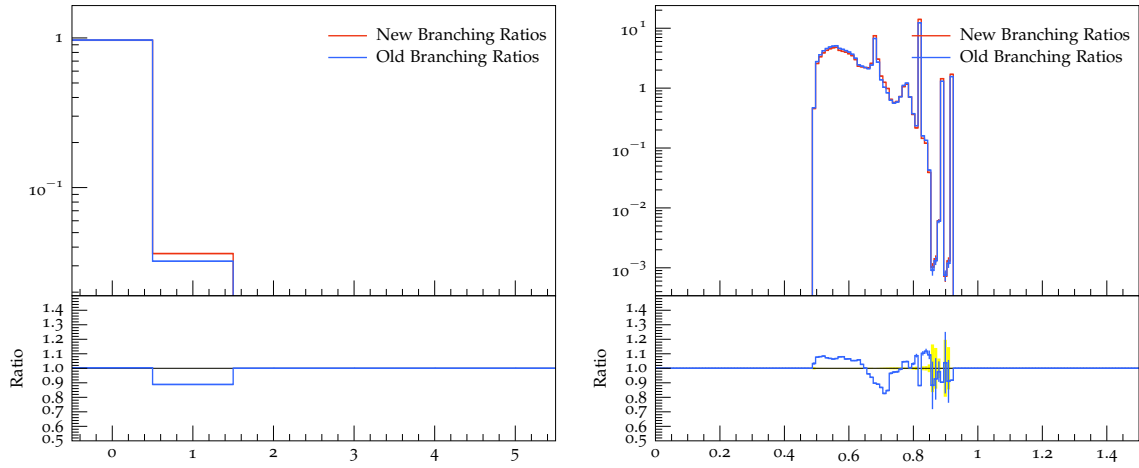
Figure A.21: multiplicity and energy spectrum of the π^+

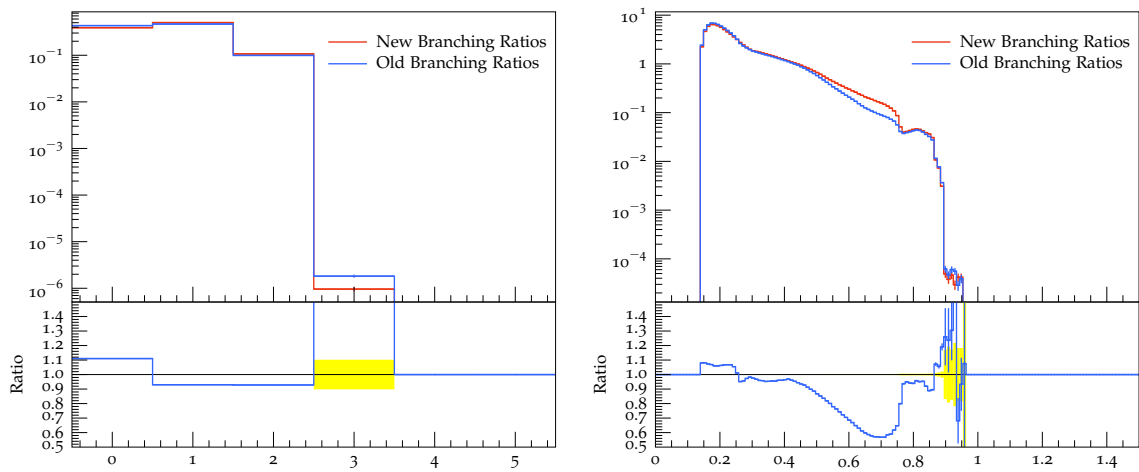**Figure A.22:** multiplicity and energy spectrum of the K^+

Figure A.23: multiplicity and energy spectrum of the π^-
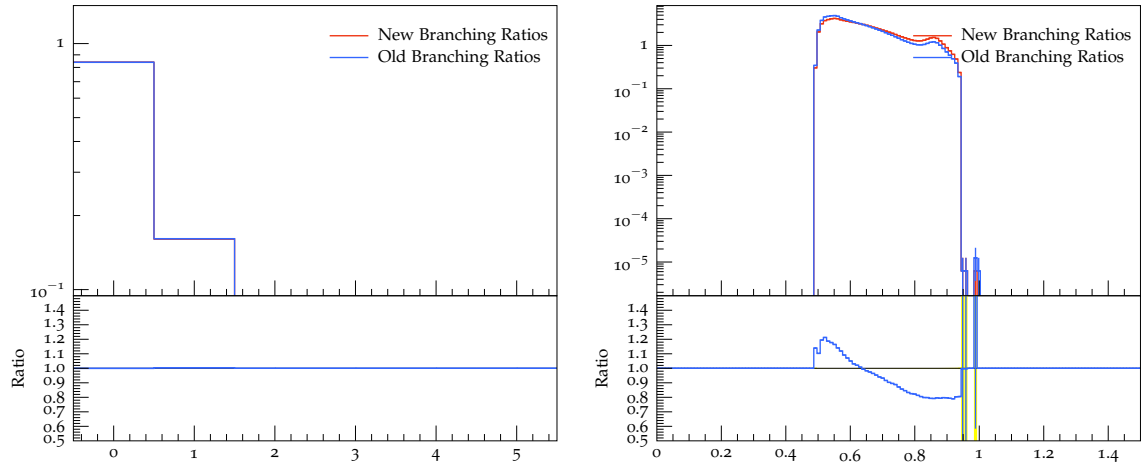
Figure A.24: multiplicity and energy spectrum of the K^-

Erklärung

Hiermit erkläre ich, dass ich diese Arbeit im Rahmen der Betreuung am Institut für Kern- und Teilchenphysik ohne unzulässige Hilfe Dritter verfasst und alle Quellen als solche gekennzeichnet habe.

Sven Schiffner
Dresden, Mai 2017